

RECEIVED: September 1, 2023

REVISED: November 30, 2023

ACCEPTED: November 30, 2023

PUBLISHED: December 18, 2023

# $P - v$ criticalities, phase transitions and geometrothermodynamics of charged AdS black holes from Kaniadakis statistics

G.G. Luciano<sup>a</sup> and E.N. Saridakis<sup>b,c,d</sup>

<sup>a</sup>Department of Chemistry, Physics and Environmental and Soil Sciences,  
Escola Politecnica Superior, Universidad de Lleida,  
Av. Jaume II, 69, 25001 Lleida, Spain

<sup>b</sup>National Observatory of Athens,  
Lofos Nymfon, 11852 Athens, Greece

<sup>c</sup>CAS Key Laboratory for Researches in Galaxies and Cosmology, Department of Astronomy,  
University of Science and Technology of China,  
Hefei, Anhui 230026, P.R. China

<sup>d</sup>Departamento de Matemáticas, Universidad Católica del Norte,  
Avda. Angamos 0610, Casilla 1280 Antofagasta, Chile

E-mail: [giuseppegaetano.luciano@udl.cat](mailto:giuseppegaetano.luciano@udl.cat), [msaridak@noa.gr](mailto:msaridak@noa.gr)

ABSTRACT: Boltzmann entropy-based thermodynamics of charged anti-de Sitter (AdS) black holes has been shown to exhibit physically interesting features, such as  $P - V$  criticalities and van der Waals-like phase transitions. In this work we extend the study of these critical phenomena to Kaniadakis theory, which is a non-extensive generalization of the classical statistical mechanics incorporating relativity. By applying the typical framework of condensed-matter physics, we analyze the impact of Kaniadakis entropy onto the equation of state, the Gibbs free energy and the critical exponents of AdS black holes in the extended phase space. Additionally, we investigate the underlying micro-structure of black holes in Ruppeiner geometry, which reveals appreciable deviations of the nature of the particle interactions from the standard behavior. Our analysis opens up new perspectives on the understanding of black hole thermodynamics in a relativistic statistical framework, highlighting the role of non-extensive corrections in the AdS black holes/van der Waals fluids dual picture.

KEYWORDS: Black Holes, Classical Theories of Gravity

ARXIV EPRINT: [2308.12669](https://arxiv.org/abs/2308.12669)

---

## Contents

<b>1</b>	<b>Introduction</b>	<b>1</b>
<b>2</b>	<b><math>P - V</math> criticality of van der Waals fluids</b>	<b>4</b>
<b>3</b>	<b>Kaniadakis thermodynamics of charged AdS black holes</b>	<b>6</b>
3.1	Heat capacity and critical point	12
3.2	$P - v$ diagram	15
3.3	Gibbs free energy	16
3.4	Behavior near the critical point	17
3.5	Sparsity of black hole radiation	20
<b>4</b>	<b>Geometrothermodynamics of charged AdS black holes</b>	<b>21</b>
<b>5</b>	<b>Conclusions and discussion</b>	<b>23</b>

---

## 1 Introduction

It is widely believed that black hole (BH) physics provides a promising arena to explore the quantum nature of gravity. After the pioneering discovery that BHs behave as thermodynamic systems [1, 2], the study of their properties has received a boost of new interest, and insights emerged toward the unification of general relativity, quantum theory and statistical physics [3–5]. Yet, although BH dynamics can be fully described by a small number of classical parameters (namely mass, angular momentum and charge — *no hair theorem*), the microscopic degrees of freedom responsible for the thermal behavior of BHs have not yet been adequately identified [6].

The development of thermodynamic geometry (geometrothermodynamics) based on Weinhold [7] and Ruppeiner [8, 9] formalisms is an effort to extract, phenomenologically or qualitatively, the microscopic interaction information of a given system from the axioms of thermodynamics. The core idea is that, in ordinary thermodynamic systems, the curvature of Weinhold and Ruppeiner metrics is related to the nature of interactions among the underlying particles. For systems where the micro-structures interact attractively, the curvature scalar carries a negative sign, whereas it is positive for predominantly repulsive forces. Moreover, the metric is flat for non-interacting systems — such as the ideal gas — or systems where interactions are perfectly balanced. This scheme has been tested for a wide number of statistical physical models [9]. Interestingly enough, recent studies have revealed that it is feasible for BHs too [10–19], providing an empirical tool to access the microstructure of BHs from their macroscopic knowledge, despite the absence of a quantum gravitational theory.

Black holes in anti-de Sitter (AdS) spacetimes have been thoroughly studied in the last decades due to their applications in holography [20]. The observation that asymptotically AdS BHs can be described by dual thermal field theory has motivated a parallel study with condensed matter systems. This has led to the discovery of first order phase transitions in BHs [21–23] that resemble in many aspects the liquid-gas change of phase of van der Waals fluids [24–26]. A constitutive ingredient of this picture is the (negative) cosmological constant  $\Lambda$ , which is identified as pressure and included in the first law of BH thermodynamics alongside its conjugate quantity — the thermodynamic volume [27, 28]. The ensuing *extended phase space* allows to formulate the  $P = P(V, T)$  equation of state and study the critical behavior of AdS BHs [28, 29]. Recent applications have been considered for rotating BHs [30] and Conformal Field Theory states that are dual to neutral singly-spinning asymptotically AdS BHs in  $d$ -bulk spacetime dimensions [31].

A subtle concept in BH physics is thermodynamic entropy. According to the holographic principle [32, 33] BHs could store information at the event horizon like holograms. In the standard Boltzmann-Gibbs statistics, this behavior is encoded by the Bekenstein-Hawking formula, which states that BH entropy scales like the surface area

$$S_{\text{BH}} = \frac{A_{bh}}{A_0}, \tag{1.1}$$

where  $A_0$  is the Planck area.<sup>1</sup> Clearly, this is an unconventional scaling. Indeed, if BHs are physically identified with their event horizon surface, they can be then regarded as genuine  $(2 + 1)$ -dimensional systems and  $S_{\text{BH}}$  is with the correct (extensive) thermodynamic entropy. However, if BHs are to be considered as  $(3 + 1)$ -dimensional objects (as arguably more natural in a  $(3 + 1)$ -dimensional description of the spacetime background), the area scaling would violate thermodynamic extensivity. Thus, Boltzmann-Gibbs theory may not be the appropriate framework for studying the thermodynamics of BHs, and a generalized non-additive entropy notion [34] or a quasi-homogeneous black hole thermodynamics [35] could be needed for such non-standard systems.

To better understand the intimate nature of BH entropy, several extensions of Boltzmann-Gibbs statistics have been considered in literature, motivated by either gravitational considerations (Tsallis [34, 36], Barrow [37] and more generalized [38] entropies) or information theory (Rényi [39] and Sharma-Mittal [40] entropies). Predictions of these models have been tested in cosmology [41–46] and quantum physics [47–50]. Recently, a non-extensive generalization inspired by the symmetries of the relativistic Lorentz group has been proposed by Kaniadakis [51–55] based on the modified entropy

$$S_\kappa = - \sum_i n_i \ln_\kappa n_i, \tag{1.2}$$

---

<sup>1</sup>We adopt units where the reduced Planck’s constant  $\hbar$ , the speed of light  $c$ , the gravitational constant  $G$ , the Boltzmann constant  $k_b$  and some reference charge  $q_p$  (eventually the Planck charge) are equal one. This, in turn, amounts to setting the Planck mass, length, time, temperature and charge as reference quantities. In this units setup, which will be simply referred to as Planck units, it is understood that all masses, lengths, times, temperatures and charges, as well as derived units, are dimensionless, since they should be thought of as being rescaled with respect to their corresponding reference quantities at Planck scale. For instance, we shall implicitly mean that  $r_+$ ,  $M$  and  $Q$  denote the ‘normalized’ BH horizon radius  $r_+ \equiv r_{\text{phys}}/l_p$ , mass  $M = M_{\text{phys}}/m_p$  and charge  $Q = Q_{\text{phys}}/q_p$ , respectively.

where the  $\kappa$ -deformed logarithm is defined by

$$\ln_{\kappa} x \equiv \frac{x^{\kappa} - x^{-\kappa}}{2\kappa}. \quad (1.3)$$

The generalized Boltzmann factor for the  $i$ -th microstate is

$$n_i = \alpha \exp_{\kappa}[-\beta (E_i - \mu)], \quad (1.4)$$

where

$$\exp_{\kappa}(x) \equiv \left( \sqrt{1 + \kappa^2 x^2} + \kappa x \right)^{1/\kappa}, \quad (1.5)$$

$$\alpha = [(1 - \kappa)/(1 + \kappa)]^{1/2\kappa}, \quad (1.6)$$

$$1/\beta = \sqrt{1 - \kappa^2} T, \quad (1.7)$$

with  $T$  and  $\mu$  being the temperature and chemical potential of the system, respectively.

Deviations from Boltzmann-Gibbs statistics are quantified by the dimensionless parameter  $-1 < \kappa < 1$ . The classical framework is, however, recovered in the  $\kappa \rightarrow 0$  limit. Besides theoretical arguments, we emphasize that phenomenological evidences for Kaniadakis statistics come from the high-quality agreement between the modified distribution (1.4) and the observed power-law tailed spectrum of cosmic rays [52].

One can show that, for the case of BHs, the dimensionless Kaniadakis entropy (1.2) can be cast as [56–59]

$$S_{\kappa} = \frac{1}{\kappa} \sinh(\kappa S_{\text{BH}}). \quad (1.8)$$

We mention here that, since the above expression is an even function of  $\kappa$ , i.e.  $S_{\kappa} = S_{-\kappa}$ , in the following we shall restrict to the  $\kappa \geq 0$  domain.

Kaniadakis entropy in the form (1.8) has been mostly used for holographic applications and, in particular, to infer corrections brought about in the Friedmann equations [57–61] (see also [56] for a recent review). In the light of the gravity-thermodynamic conjecture, preliminary studies in BH thermodynamics have been considered in [64] by computing the  $\kappa$ -deformed temperature and heat capacity in the context of generalized Heisenberg relations [65, 66]. Nevertheless, to the best of our knowledge, a dedicated analysis of BH geometrothermodynamics and critical phenomena in Kaniadakis statistics has not yet been conducted.

Starting from the above premises, in this work we address the thermodynamics of AdS BHs from the Kaniadakis entropy perspective. We investigate the impact of eq. (1.8) on small-large BH phase transitions and critical exponents by exploiting the language of condensed matter physics. In this sense, the main effort here is to lay the foundation towards formulating BH thermodynamics in a fully relativistic statistical context. We then examine the underlying microstructure of BHs in Ruppeiner geometry, which reveals predominantly repulsive intermolecular forces. In line with the discussion of [67–73], our analysis shows that the development of BH thermodynamics based on a non-extensive entropy notion involves a consistent redefinition of all other thermodynamic quantities, including the Hawking temperature and thermodynamic energy.

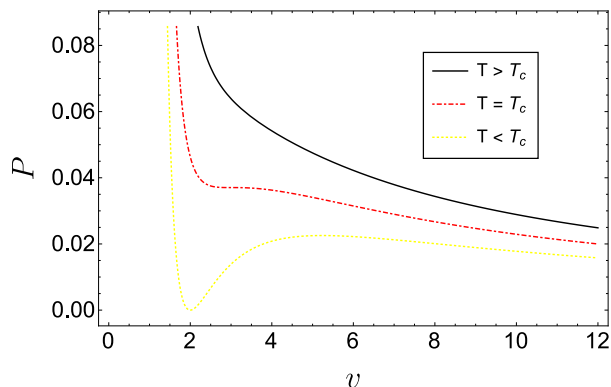


**Figure 1.**  $P - v$  diagram of van der Waals fluids. The red dot-dashed line indicates the critical isotherm at  $T = T_c$ . We have set  $a = b = 1$  (online colors).

The structure of the work is as follows: for later comparison with physics of BHs, the next section is devoted to review phase transitions and critical phenomena of van der Waals fluids. In section 3 we study thermodynamics of charged AdS BHs in Kaniadakis statistics, while section 4 concerns geometrothermodynamic analysis. Conclusions and perspectives are finally discussed in section 5.

## 2 $P - V$ criticality of van der Waals fluids

In this section we basically follow the analysis of Kubiznak and Mann [26]. To keep consistency with their notation and results, we here use the same conventions as in [26]. It is well-known that Van der Waals model provides an effective description of real interacting fluids and liquid-gas phase transitions. The characteristic equation is

$$\left(P + \frac{a}{v^2}\right)(v - b) = T, \quad (2.1)$$

where  $v = V/N$ ,  $N$ ,  $V$ ,  $P$  and  $T$  denote the specific volume, number of constituents, global volume, pressure and temperature of the van der Waals system, respectively. The positive constant  $a$  and  $b$  quantify the attraction and finite size of the molecules in the fluid.

The qualitative behavior of  $P - V$  isotherms is displayed in figure 1. It can be seen that the *critical point* of the liquid-gas phase transition occurs when  $P(v)$  has an inflection point, which is obtained by imposing

$$\left(\frac{\partial P}{\partial v}\right)_T = \left(\frac{\partial^2 P}{\partial v^2}\right)_T = 0. \quad (2.2)$$

In this way, we obtain

$$v_c = 3b, \quad T_c = \frac{8a}{27b}, \quad P_c = \frac{a}{27b^2}, \quad (2.3)$$

for the critical volume, temperature and pressure, respectively. It is immediate to check that

$$P_c v_c / T_c = 3/8, \quad (2.4)$$

which is a universal number predicted for all fluids (independently of the constants  $a$  and  $b$ ).

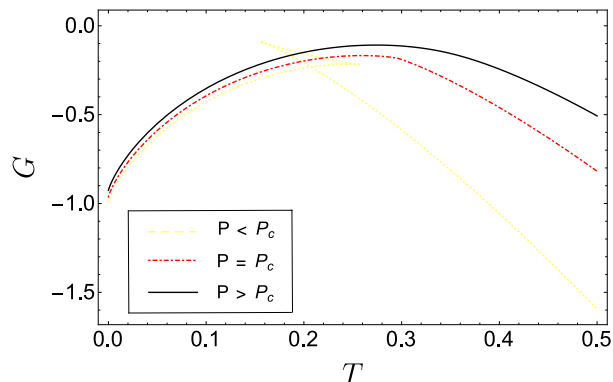


**Figure 2.** Gibbs free energy  $G$  versus temperature  $T$  for various pressures  $P$ , for van der Waals fluids. The red dot-dashed line indicates the critical isobar at  $P = P_c$  (online colors).

To gain more insights on the phase transitions of van der Waals fluids, let us introduce the (specific) Gibbs free energy,  $G = G(P, T)$ . For fixed  $N$ , this is given by [26]

$$G(T, P) = -T \left\{ 1 + \log \left[ \frac{(v - b) T^{\frac{3}{2}}}{\lambda} \right] \right\} - \frac{a}{v} + Pv, \quad (2.5)$$

where  $v$  is to be understood as a function of pressure and temperature through eq. (2.1), while  $\lambda$  is a (dimensional) specific constant of the gas. The behavior of  $G$  versus  $T$  is shown in figure 2 for different  $P$ . Below the critical pressure (yellow dotted curve), it exhibits the “swallow-tail” shape characteristic of first order phase transitions from liquid to gas. Such a feature disappears for  $P > P_c$  (black solid line).

The behavior of the physical variables near the critical point is quantitatively described by the critical exponents. Following [26], we introduce

$$t = \frac{T - T_c}{T_c} = \tau - 1, \quad \phi = \frac{v - v_c}{v_c} = \nu - 1. \quad (2.6)$$

The basic critical exponents  $\alpha, \beta, \gamma$  and  $\delta$  are then defined as follows (for computational details, see [74]):

- $\alpha$  governs the dynamics of the specific heat at constant volume  $C_v$  according to  $C_v = T \left( \frac{\partial S}{\partial T} \right)_v \propto |t|^{-\alpha}$ . By explicit computation, one sees that  $C_v$  does not depend on  $t$ , which implies  $\alpha = 0$ .
- $\beta$  describes the behavior of the order parameter  $\eta = v_g - v_l$  for a given isotherm as  $\eta \propto |t|^\beta$ , where  $v_{g,l}$  denote the volume of the gas and liquid phases, respectively. From the equation of corresponding states for van der Waals fluids and the Maxwell’s equal area law, it follows that  $\beta = 1/2$ .
- $\gamma$  measures the isothermal compressibility  $\kappa_T$  of the fluid in compliance with  $\kappa_T = -\frac{1}{v} \left( \frac{\partial v}{\partial P} \right)_T \propto |t|^{-\gamma}$ . By using again the equation of corresponding states, one finds  $\gamma = 1$ .
- $\delta$  controls the difference  $|P - P_c|$  on the critical isotherm  $T = T_c$  according to  $|P - P_c| \propto |v - v_c|^\delta$ . The study of the shape of the critical isotherm gives  $\delta = 3$ .

The above considerations provide the basics of our next analysis. Specifically, we elaborate on the correspondence between phase transitions of BHs and van der Waals fluids within Kaniadakis framework, with focus on the  $\kappa$ -deformed analogues of eq. (2.1)–(2.6).

### 3 Kaniadakis thermodynamics of charged AdS black holes

The general static and spherically symmetric metric that describes (3 + 1)-dimensional charged AdS BHs is given by [75]

$$ds^2 = -f(r)dt^2 + f(r)^{-1}dr^2 + r^2d\Omega^2, \tag{3.1}$$

where  $d\Omega^2 = d\theta^2 + \sin^2\theta d\phi^2$  is the angular part of the metric on the two-sphere. Here, we have defined<sup>2</sup>

$$f(r) = 1 - \frac{2M}{r} + \frac{Q^2}{r^2} + \frac{r^2}{l^2}, \tag{3.2}$$

where  $M, Q, l$  are the normalized mass, electric charge and AdS radius of the BH (see footnote 1). The latter is related to the (negative) cosmological constant by

$$\Lambda = -\frac{3}{l^2}. \tag{3.3}$$

Clearly, for  $Q = 0$  and  $l \gg r$ , eq. (3.1) reduces to the well-known Schwarzschild metric. Additionally, the normalized event horizon  $r_+$  of the geometry (3.1) corresponds to the largest root of  $f(r) = 0$ . One can use this solution to express the BH mass as

$$M(r_+) = \frac{r_+}{2} + \frac{Q^2}{2r_+} + \frac{r_+^3}{2l^2}. \tag{3.4}$$

Before we proceed further, it is worth performing dimensional analysis, translating the above relation to physical units. Taking footnote 1 into account, we naturally get

$$\frac{M_{\text{phys}}}{m_p} = \frac{r_{+\text{phys}}}{2l_p} + \frac{Q_{\text{phys}}^2}{q_p^2} \frac{l_p}{2r_{+\text{phys}}} + \frac{r_{+\text{phys}}^3}{l_p^3} \frac{l_p^2}{2l_{\text{phys}}^2},$$

where the subscript *phys* indicates correct dimensional quantities in the international system. The above equation is dimensionally consistent, since all the ratios in the left and right sides are pure numbers. All other equations in the manuscript either follow from eq. (3.4) or can be treated by using the same prescription.

The normalized surface area  $A_{bh}$  of the BH horizon reads

$$A_{bh} = 4\pi r_+^2. \tag{3.5}$$

Returning to our system of Planck units, the Bekenstein-Hawking entropy based on the classical Boltzmann-Gibbs statistics obeys

$$S_{\text{BH}} = \frac{A_{bh}}{4} = \pi r_+^2. \tag{3.6}$$

---

<sup>2</sup>Following the study of [76–80] in Tsallis and Barrow frameworks, here we assume that Kaniadakis model only modifies BH entropy, while leaving the field equations of the theory unaffected. A comprehensive analysis of BH thermodynamics involving an ab initio derivation of a lagrangian driven by the Kaniadakis entropic index is reserved for the future.

Notice that, according to the set of units we are using, this is a dimensionless measure of the BH horizon entropy, namely the entropy rescaled by the number of bits associated with a Planck-size area.

As discussed in the Introduction, due to the area scaling of BH entropy, arguments from multiple perspectives suggest that Boltzmann-Gibbs statistics may not be the appropriate context for studying the thermodynamics of BHs. In particular, in a relativistic scenario eq. (3.6) is expected to be generalized to Kaniadakis entropy (1.8), which we rewrite here by dropping for simplicity the index  $\kappa$

$$S = \frac{1}{\kappa} \sinh(\kappa S_{\text{BH}}) . \tag{3.7}$$

Some comments are in order: first, it should be stressed that, although the Bekenstein-Hawking entropy (3.6) is commonly used in the relativistic theory, it is essentially classical. Indeed, according to the maximum entropy principle, it is maximized when a given system in thermodynamic equilibrium is in a state described by the Maxwell-Boltzmann distribution, which has the classical Boltzmann-Gibbs statistics as a natural frame. At first glance, one might be tempted to generalize the Maxwell-Boltzmann factor to the Maxwell-Jüttner distribution, which provides the first effort to construct a relativistic statistical theory [81]. However, this model is developed by naively replacing the classical energy-velocity relation with its relativistic generalization into the Maxwell-Boltzmann distribution. In so doing, one obtains a hybrid distribution that still maximizes the classical Boltzmann-Gibbs-Shannon entropy. On the other hand, the non-extensive Kaniadakis entropy (3.7) stems from the generalized distribution (1.4), which is built out from an ab initio relativistic statistical framework — Kaniadakis statistics. As shown in refs. [51–55], the latter statistics is relativistic in the sense that it respects the relativistic invariance and includes the relativistic form of the energy-momentum relation. We thus believe that the present analysis provides a first relevant step toward a comprehensive extension of black hole thermodynamics to a general relativistic entropic scenario.

Furthermore, we observe that  $S$  is a monotonically increasing function of  $S_{\text{BH}}$  and, thus, of the horizon radius  $r_+$ . Moreover, in order to provide analytical solutions, it proves sometimes convenient to perform Taylor expansions of eq. (3.7) to the leading order [58, 82]. This assumption is substantiated by the agreement between theoretical predictions and phenomenological implications of Kaniadakis model, which is obtained for  $\kappa = 0.2165$  in high-energy particle physics [52]. Note that in cosmological applications,  $\kappa$  is found to be much closer to zero [60–62], for instance  $\kappa \sim \mathcal{O}(10^{-125})$  from Baryon acoustic oscillations measurements. On the other hand, small but still appreciable effects are expected to arise in the astrophysical context, which is the framework we are actually considering here. For example, constraints on  $\kappa$  have been set in [63] by studying the impact of Kaniadakis entropy on the physics of galaxy clusters. Although the classical Boltzmann-Gibbs statistics is well-consistent with data, non-Gaussian effects cannot be completely ruled out, constraining  $0 \leq \kappa \leq 0.034$  at  $1\sigma$  confidence level. Since, to the best of our knowledge, this is one of the most accurate observational constraints on Kaniadakis entropy within the realm of astrophysics, in what follows we stick to this bound as for the adopted values of the entropic parameter  $\kappa$ . Additionally, we shall retain the exact expression of  $S$  as far as possible,



resorting to the leading order approximation of eq. (3.7)

$$S = S_{\text{BH}} + \frac{S_{\text{BH}}^3 \kappa^2}{6} + \mathcal{O}(\kappa^4), \quad (3.8)$$

when necessary.

For  $\kappa \sim \mathcal{O}(10^{-2})$ , in order for the above expansion to make sense, we need to restrict to  $S_{\text{BH}} \ll \mathcal{O}(10^2)$ . In compliance with these caveats, we shall fix  $\kappa$  and  $S_{\text{BH}}$  in such a way that the ratio between the leading order correction and standard term is small enough and the expansion (3.8) can be reasonably performed. The study of Kaniadakis effects on BH thermodynamics for larger values of entropies (i.e. for very large BHs) requires developing exact computations beyond the leading order expansion (3.8). Because of cumbersome technicalities, this aspect is reserved for future investigation. In spite of this restriction, we would however remark that our analysis still highlights suggestive results, such as a non-trivial impact of non-extensive Kaniadakis entropy on BH phase transitions, the critical parameters, the generalized law of corresponding states, the behavior near the critical point and the thermodynamic (microstructure) interaction properties.

The thermodynamic picture of AdS BHs is completed by the introduction of an extended phase space, where the pressure is identified with the cosmological constant and the thermodynamic volume with its conjugate quantity, i.e.

$$P = -\frac{\Lambda}{8\pi} = \frac{3}{8\pi l^2}, \quad (3.9)$$

$$V = \left(\frac{\partial M}{\partial P}\right)_{S,Q} = \frac{4}{3}\pi r_+^3, \quad (3.10)$$

respectively. Equipped with these new definitions, it is easy to check that BHs still obey the first law of thermodynamics [26]

$$dM = TdS + \varphi dQ + VdP, \quad (3.11)$$

and Smarr relation

$$M = 2(TS - VP) + \Phi Q, \quad (3.12)$$

where

$$T = \left(\frac{\partial M}{\partial S}\right)_{P,Q}, \quad \Phi = \left(\frac{\partial M}{\partial Q}\right)_{S,P}, \quad (3.13)$$

are the normalized temperature and electric potential, respectively.

Using the standard thermodynamic machinery, we now have all the ingredients to compute the necessary BH thermodynamic variables. Since BH phase transitions have been shown to occur in the canonical (fixed charge) ensemble [21, 22], we conduct our analysis in this framework. As a first step, we express the mass parameter (3.4) in terms of the Kaniadakis entropy, using the relation (1.8). This gives

$$M(S) = \frac{(\pi l Q \kappa)^2 + \pi l^2 \kappa \operatorname{ash}(\kappa S) + \operatorname{ash}^2(\kappa S)}{2\pi^{\frac{3}{2}} l^2 \kappa^{\frac{3}{2}} \operatorname{ash}^{\frac{1}{2}}(\kappa S)}, \quad (3.14)$$

where we have introduced the shorthand notation

$$\operatorname{ash}(x) \equiv \operatorname{arcsinh}(x). \quad (3.15)$$

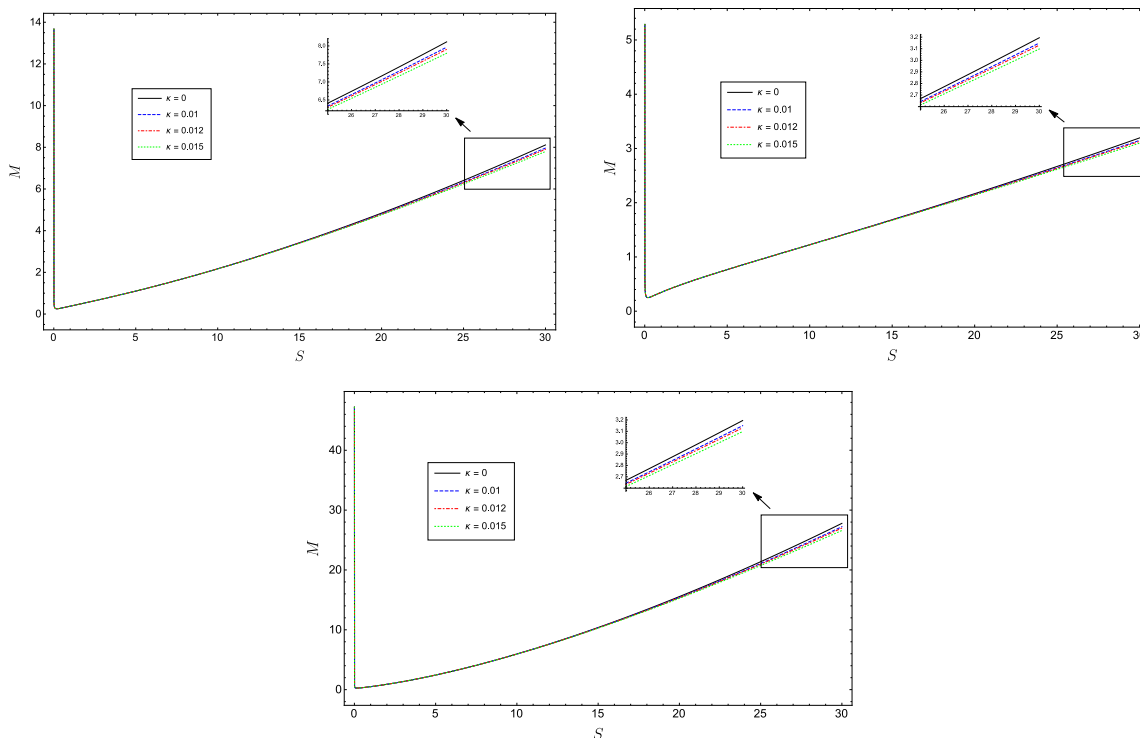


**Figure 3.** The mass parameter  $M$  versus the entropy  $S$  for various values of  $\kappa$  and  $l = l_c$  fixed through the critical condition (3.26) (upper panel),  $l = 2l_c$  (middle panel) and  $l = 0.5l_c$  (lower panel) (online colors).

One can verify that the limit for  $\kappa \rightarrow 0$  of eq. (3.14) reproduces the standard expression of  $M$  for charged AdS BHs (solid black lines in figure 3).

The behavior of the  $\kappa$ -deformed mass (3.14) versus  $S$  is shown in figure 3 for various  $\kappa$ ,  $l$  and fixed  $Q = 0.25$ . As we can see,  $M$  remains positive and shows an initially decreasing behavior (evaporation phase of the BH), followed by a later growth (absorption process). While leaving the initial stage of the evolution nearly unaffected, Kaniadakis entropy influences the final growth rate of  $M$ , with lower  $\kappa$  corresponding to a faster growth and vice-versa. For the sake of comparison with recent literature, we emphasize that a similar result has been found in the context of quantum gravity-induced deformations of Boltzmann-Gibbs entropy [78] and in non-linear electrodynamics and the Einstein-massive gravity [83].

The usage of eq. (3.14) along with the first law of thermodynamics (3.11) allows us to derive the  $\kappa$ -temperature of the thermal radiation emitted by BHs as

$$\begin{aligned}
 T(S) &= \left( \frac{\partial M}{\partial S} \right)_P \tag{3.16} \\
 &= \frac{-(\pi l Q \kappa)^2 + \pi l^2 \kappa \operatorname{ash}(\kappa S) + 3 \operatorname{ash}^2(\kappa S)}{4\pi^{\frac{3}{2}} l^2 \left[ (1 + \kappa^2 S^2) \kappa \operatorname{ash}^3(\kappa S) \right]^{\frac{1}{2}}},
 \end{aligned}$$

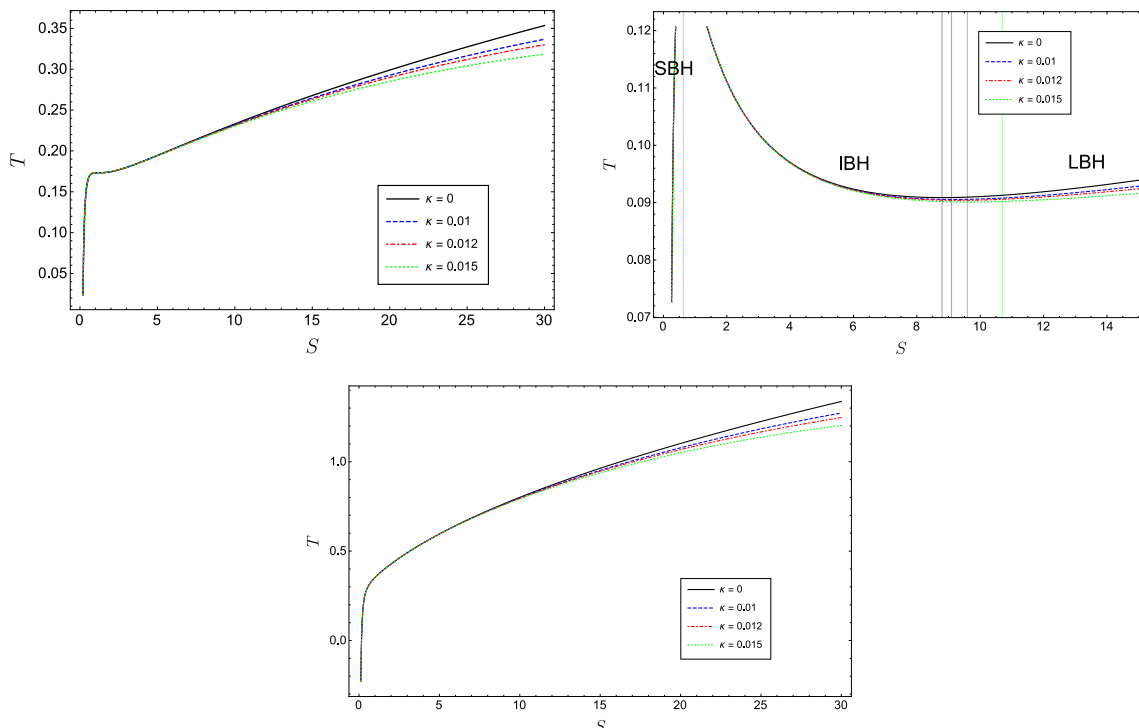


**Figure 4.** The temperature  $T$  versus the entropy  $S$  for various values of  $\kappa$  and  $l = l_c$  fixed through the critical condition (3.26) (upper panel),  $l = 2l_c$  (middle panel) and  $l = 0.5l_c$  (lower panel). In order to properly display all features of the  $T - S$  diagrams, in the middle panel we have slightly restricted the domain of  $S$ . The vertical solid lines in the middle panel separate Region II — Intermediate Black Hole (IBH) — from Region I — Small Black Hole (SBH) — and Region III — Large Black Hole (LBH) — see text (online colors).

which, in the limit of  $\kappa \rightarrow 0$ , still recovers the usual result (solid black line in figure 4)

$$T_{\kappa \rightarrow 0}(S) = \frac{3S^2 + \pi l^2 (S - \pi Q^2)}{4\pi^{\frac{3}{2}} l^2 S^{\frac{3}{2}}}. \tag{3.17}$$

We further notice that the above relation has the well-defined Schwarzschild limit  $T = 1/(4\pi r_+)$  for  $Q \rightarrow 0$  and  $l \rightarrow \infty$ .

Equation (3.16) is plotted as a function of  $S$  in figure 4 for various  $\kappa, l$  and fixed  $Q$  as before. The points where the slope of the  $T - S$  graphs vanishes are of special interest, as they signal a potentially critical behavior of BHs (see the next section for more quantitative discussion). From figure 4, we see that  $T$  exhibits one, two or no stationary points, depending on the value of  $l$  (or, equivalently, of  $P$ ). Specifically, from the upper panel we observe that  $T$  has one stationary point as far as  $S$  is kept small enough to comply with the condition (3.8). Notice also that this point occurs for Planck-size BHs for the specific setup of model parameters. It is easy to check that it shifts toward higher  $S$  for higher values of  $Q$ .

An interesting behavior is also exhibited as  $S$  increases. Indeed, eq. (3.16) reveals that, while the standard BH temperature  $T_{\kappa=0}$  is a monotonically increasing function that blows

up asymptotically,  $T_{\kappa \neq 0}$  starts decreasing for  $S$  large enough and ultimately vanishes. We thus infer that sufficiently large Kaniadakis AdS BHs should appear colder than standard AdS BHs of equal size. Such a behavior could signal the emergence of suggestive new physics in this regime with respect to the  $\kappa = 0$  case. However, a detailed analysis of this feature lies outside the applicability of the present formalism. Indeed, although we are able to provide the exact expressions of the  $\kappa$ -modified temperature, our thermodynamic considerations on the phase structure and transitions of AdS black holes make sense as far as the leading order approximation (3.8) remains meaningful. Such an approximation is in fact needed to derive the analytic expressions of the critical parameters and explore the behavior near the critical point (see the discussion in section 3.1). Therefore, a proper treatment of this behavior requires going beyond the leading order approximation and possibly develop exact analytic calculations.

On the other side, from the lower panel of figure 4, we observe that  $T$  increases monotonically and has no stationary point for entropies consistent with eq. (3.8). As discussed above, the study of Kaniadakis BH thermodynamics for large values of  $S$  might reveal non-trivial behaviors. However, it breaks down the approximation (3.8) and will be thus discussed in a future analysis.

Finally, the middle panel of figure 4 shows that  $T$  increases for small (Region I — Small Black Hole (SBH)) and large (Region III — Large Black Hole (LBH)) values of the entropy, while it decreases in the intermediate domain (Region II — Intermediate Black Hole (IBH)). These regions are separated by two stationary points, which have been marked by vertical solid lines for better visual clarity. Effects of Kaniadakis entropy manifest through a variation of the width of the IBH region, with higher  $\kappa$  yielding a larger IBH domain and vice-versa. Below, we shall see this behavior of  $T - S$  graph is peculiar to a first-order phase transition between SBH and LBH, which resembles in many aspects the liquid-gas change of phase of van der Waals fluids.

In this picture, the larger amplitude of the IBH domain for higher  $\kappa$  can be understood in terms of the non-extensive character of Kaniadakis entropy by looking at the BH structure on a molecular level (see section 4). For higher  $\kappa$ , indeed, the repulsive forces among BH microstructures tend to be weaker, at least in the first stage of BH evolution, which implies a slowed small-to-large phase transition of BH. To carry on the similarity with van der Waals-like systems (where, however, interparticle forces are mostly attractive), one can think of a Kaniadakis BH as a fluid with stronger attraction for larger  $\kappa$ . In this case, more heat is necessary to the internal molecules to overcome these attractive interactions, which results in a delayed liquid-gas change of phase. Again, we here mention that some non-trivial behavior could be exhibited for very large entropies. This regime is however outside the scope of this work.

Finally, regardless of the value of  $l$ , the condition  $T(S_0) = 0$  gives the *physical limitation point of BHs*. Indeed, for  $S < S_0$  the temperature becomes negative, which means this region is physically inaccessible.

Before moving on, we remark that the employment of generalized (non-extensive) entropies like that in eq. (1.8) leads to multiplicity in the temperature value of BHs. In [71] it has been observed that three different scenarios may occur, depending on the assumed

energy and temperature definitions. In compliance with [77, 78], here we are considering the energy definition of GR, the first law of thermodynamics and the thermodynamic temperature definition as fundamental. An alternative viewpoint has been adopted in [71], based on the assumption that the Hawking temperature must be kept unaffected. It is interesting to explore whether, and if so, how the present results get modified in such a complementary approach. Investigation along this direction is left for future work.

### 3.1 Heat capacity and critical point

With the help of the temperature (3.16), one can obtain the heat capacity at constant pressure as

$$\begin{aligned}
 C_p(S) &= T \left( \frac{\partial S}{\partial T} \right)_P \\
 &= -\frac{2}{\kappa} \left( 1 + \kappa^2 S^2 \right)^{\frac{3}{2}} \text{ash}(\kappa S) \left[ (\pi l Q \kappa)^2 - \text{ash}(\kappa S) \left( \pi l^2 \kappa + 3 \text{ash}(\kappa S) \right) \right] \\
 &\quad \times \left\{ 3 (\pi l Q \kappa)^2 \left( 1 + \kappa^2 S^2 \right) - \text{ash}(\kappa S) \left\{ \pi l^2 \kappa \left[ 1 + \kappa^2 S \left( S - 2\pi Q^2 (1 + \kappa^2 S^2)^{\frac{1}{2}} \right) \right] \right. \right. \\
 &\quad \left. \left. + \text{ash}(\kappa S) \left[ -3 + \kappa^2 S \left( -3S + 2\pi l^2 (1 + \kappa^2 S^2)^{\frac{1}{2}} \right) + 6\kappa S \text{ash}(\kappa S) \left( 1 + \kappa^2 S^2 \right)^{\frac{1}{2}} \right] \right\} \right\}^{-1},
 \end{aligned} \tag{3.18}$$

which for  $\kappa \rightarrow 0$  consistently reduces to (solid black line in figure 5)

$$C_{p,\kappa \rightarrow 0} = \frac{2\pi r_+^2 [3r_+^4 + l^2 (r_+^2 - Q^2)]}{[3r_+^4 + l^2 (3Q^2 - r_+^2)]}. \tag{3.19}$$

It is important to note that  $C_p > 0$  corresponds to local stability of BHs, while for  $C_p < 0$  even small perturbations may cause BH disappearance. Also, discontinuities potentially indicate a critical behavior of BHs.

Equation (3.18) is plotted as a function of  $S$  in figure 5 for various  $\kappa, l$  and fixed  $Q$  as before. In compliance with the discussion below eq. (3.16), it is observed that  $C_p$  has one (upper panel), two (middle panel) or no (lower panel) discontinuity, depending on the value of  $l$ . The SBH, IBH and LBH regions are clearly distinguishable from the middle panel (the vertical lines correspond to the two stationary points of the  $T - S$  graphs in the middle panel of figure 4). While SBH and LBH are thermodynamically stable ( $C_p > 0$ ), IBH is unstable ( $C_p < 0$ ). As discussed, for instance, in [26] this gives rise to a transition between the SBH and LBH “phases”. As  $l$  progressively decreases to a certain critical value (upper panel), the IMB range reduces to a point, which in turn corresponds to the single stationary point of the  $T - S$  graph in the upper panel of figure 4. By further decreasing  $l$  (lower panel),  $C_p$  is always continuous and keeps positive values. In this case, BHs are locally stable and do not undergo any transition (see also the corresponding  $T - S$  graphs in the lower panel of figure 4).

To better understand the origin of this critical value of  $l$ , we now derive the analogue of the equation of state (2.1) for BHs in the extended phase space. By using eq. (3.9)

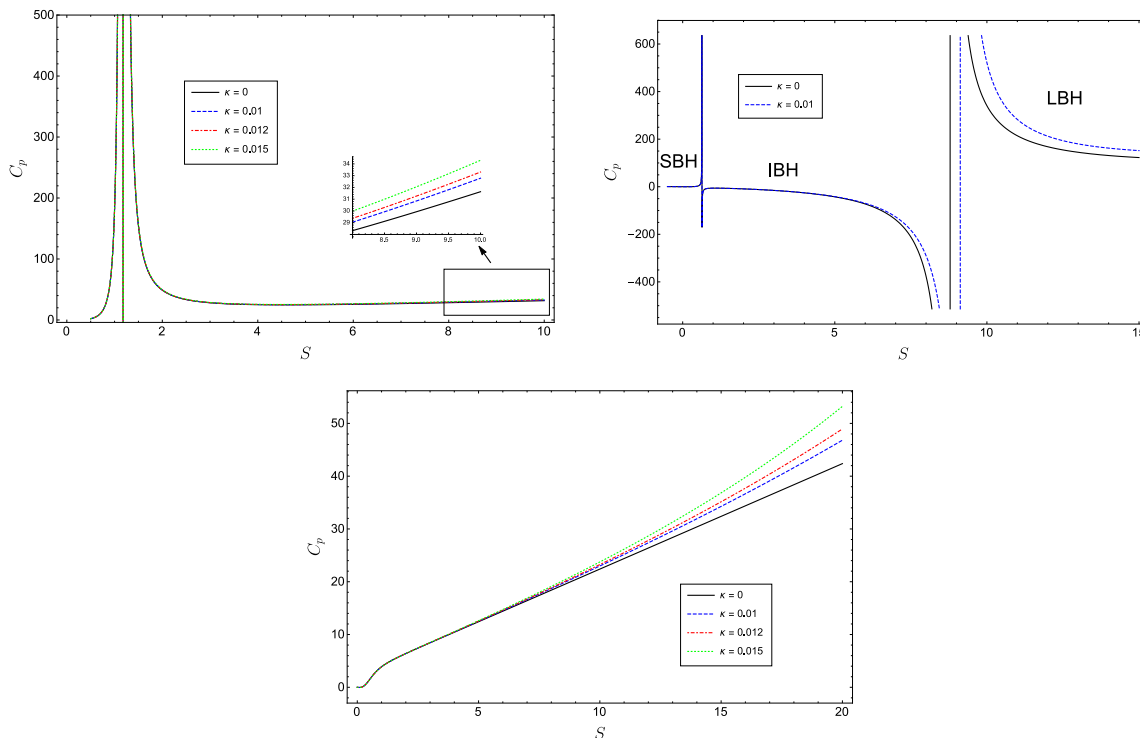


**Figure 5.** The heat capacity at constant pressure  $C_p$  versus the entropy  $S$  for various  $\kappa$  values, and for  $l = l_c$  fixed through the critical condition (3.26) (upper panel),  $l = 2l_c$  (middle panel) and  $l = 0.5l_c$  (lower panel). For visual clarity, we have only considered two values of  $\kappa$  in the middle panel (online colors).

and (3.16), after some algebra we get

$$P(r_+) = \cosh\left(\pi\kappa r_+^2\right) \frac{T}{2r_+} + \frac{Q^2}{8\pi r_+^4} - \frac{1}{8\pi r_+^2}, \quad (3.20)$$

which is now straightforward to match with the  $\kappa \rightarrow 0$  limit [26]

$$P_{\kappa \rightarrow 0}(r_+) = \frac{T}{2r_+} + \frac{Q^2}{8\pi r_+^4} - \frac{1}{8\pi r_+^2}. \quad (3.21)$$

Once more, it could be interesting translate the above relation in Planck units to physical units. Focusing on the first term in the right-side (for comparison with eq. (3.12) of [26]) and following the prescription in footnote 1, we obtain

$$P_{\text{phys}} = \cosh\left(\pi\kappa_{\text{phys}} r_{+\text{phys}}^2 \frac{k_b}{l_p^2}\right) \frac{T_{\text{phys}}}{2r_{+\text{phys}}} \frac{k_b}{l_p^2} + \dots,$$

which is dimensionally self-consistent and coincides with eq. (3.12) of [26] for  $\kappa_{\text{phys}} \rightarrow 0$ .

To directly compare eq. (3.20) with eq. (2.1), we follow [26] and identify the horizon radius  $r_+$  with the specific volume of van der Waals fluid as [26]

$$v = 2r_+. \quad (3.22)$$

In this way, we obtain

$$P(v) = \cosh\left(\frac{\pi\kappa v^2}{4}\right) \frac{T}{v} + \frac{2Q^2}{\pi v^4} - \frac{1}{2\pi v^2}. \quad (3.23)$$

As discussed for van der Waals fluids, the critical point of phase transitions can be derived from the conditions (2.2). However, analytical expressions for the critical specific volume, temperature and pressure can only be obtained to the leading order in  $\kappa$ . In this approximation, we are allowed to write down

$$v_c = 2\sqrt{6}Q + 144\sqrt{6}\pi^2 Q^5 \kappa^2 + \mathcal{O}(\kappa^3), \quad (3.24)$$

$$T_c = \frac{1}{3\sqrt{6}\pi Q} + 3\sqrt{6}\pi Q^3 \kappa^2 + \mathcal{O}(\kappa^3), \quad (3.25)$$

$$P_c = \frac{1}{96\pi Q^2} + 2\pi Q^2 \kappa^2 + \mathcal{O}(\kappa^3), \quad l_c^2 = \frac{3}{8\pi P_c}, \quad (3.26)$$

all reducing to the standard critical expressions for  $\kappa \rightarrow 0$  [26]. Notice that, for  $Q > 0$ , Kaniadakis corrections are positive. In particular, from eqs. (3.24) and (3.25) we infer that Kaniadakis BHs are hotter and larger than standard BHs at the critical point of phase transition. Furthermore, the relation (3.24) allows us to derive the thermodynamic volume corresponding to the critical volume  $v_c$  as

$$V_c = \frac{4}{3}\pi r_c^3 = 8\sqrt{6}\pi Q^3 + 1728\sqrt{6}\pi^3 Q^7 \kappa^2 + \mathcal{O}(\kappa^3). \quad (3.27)$$

It is worth noting that  $v_c \rightarrow 0$ , while  $T_c, P_c \rightarrow \infty$  for  $Q \rightarrow 0$  regardless of  $\kappa$ , which means that the critical transition described above is characteristic of charged BHs also in Kaniadakis entropy model (on the other hand, in [84] it has been found that AdS BHs in Gauss-Bonnet gravity undergo small-large transitions in the uncharged case too).

Interestingly enough, the critical parameters (3.24)–(3.26) satisfy the relation

$$\frac{P_c v_c}{T_c} = \frac{3}{8} + \frac{315}{4}\pi^2 Q^4 \kappa^2 + \mathcal{O}(\kappa^3). \quad (3.28)$$

We deduce that Kaniadakis entropy-based BHs slightly deviate from pure van der Waals behavior, due to the  $\kappa$ -dependent correction. The latter behavior is, however, recovered for  $\kappa \rightarrow 0$ .

Now, by introducing the re-scaled variables

$$p = \frac{P}{P_c}, \quad \nu = \frac{v}{v_c}, \quad \tau = \frac{T}{T_c}, \quad (3.29)$$

the equation of state (3.23) can be rearranged as

$$8\tau = 3\nu \left( Ap + \frac{2B}{\nu^2} \right) - \frac{D}{\nu^3}, \quad (3.30)$$

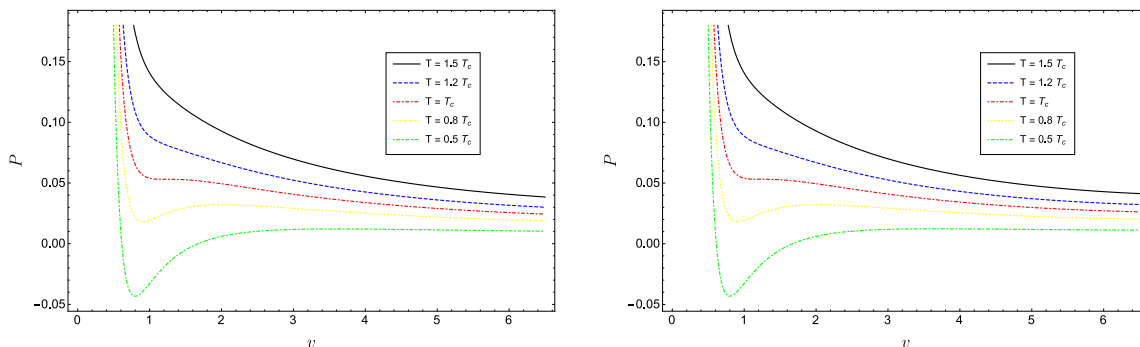


**Figure 6.**  $P - v$  diagrams for  $\kappa = 0.01$  (top panel) and  $\kappa = 0.015$  (bottom panel). In each panel, the temperature of the isotherms decreases from top to bottom. The red dot-dashed line indicates the critical isotherm at  $T = T_c$  (online colors).

where

$$\begin{aligned}
 A &= \frac{8P_c v_c}{3T_c \cosh\left(\frac{\pi\kappa v^2}{4}\right)} \\
 &= 1 + 6\pi^2 Q^4 (35 - 3\nu^4) \kappa^2 + \mathcal{O}(\kappa^3), \tag{3.31}
 \end{aligned}$$

$$\begin{aligned}
 B &= \frac{2}{3\pi T_c v_c \cosh\left(\frac{\pi\kappa v^2}{4}\right)} \\
 &= 1 - 18\pi^2 Q^4 (7 + \nu^4) \kappa^2 + \mathcal{O}(\kappa^3), \tag{3.32}
 \end{aligned}$$

$$\begin{aligned}
 D &= \frac{16Q^2}{\pi T_c v_c^3 \cosh\left(\frac{\pi\kappa v^2}{4}\right)} \\
 &= 1 - 18\pi^2 Q^4 (15 + \nu^4) \kappa^2 + \mathcal{O}(\kappa^3). \tag{3.33}
 \end{aligned}$$

Equation (3.30) has the same structure as the law of corresponding states for fluids [26]

$$8\tau = 3\nu \left( p + \frac{2}{\nu^2} \right) - \frac{1}{\nu^3}. \tag{3.34}$$

It is easy to check that this equation is correctly restored for  $\kappa \rightarrow 0$ , since  $A = B = D = 1$  in this limit.

### 3.2 $P - v$ diagram

We proceed by investigating the  $P - v$  diagrams of AdS BHs as given in eq. (3.23). These diagrams are displayed in figure 6 for various  $\kappa$ ,  $T$  and fixed  $Q$  as before. By comparison with figure 1, we see that the isotherms at  $T < T_c$  (green and yellow curves) have van der Waals-like oscillations with a local minimum and maximum. This behavior appears even more evident from the plot of the derivative of  $P$  with respect to  $v$  in figure 7, which shows that  $\partial_v P$  is continuous and varies from initially negative to positive values, and



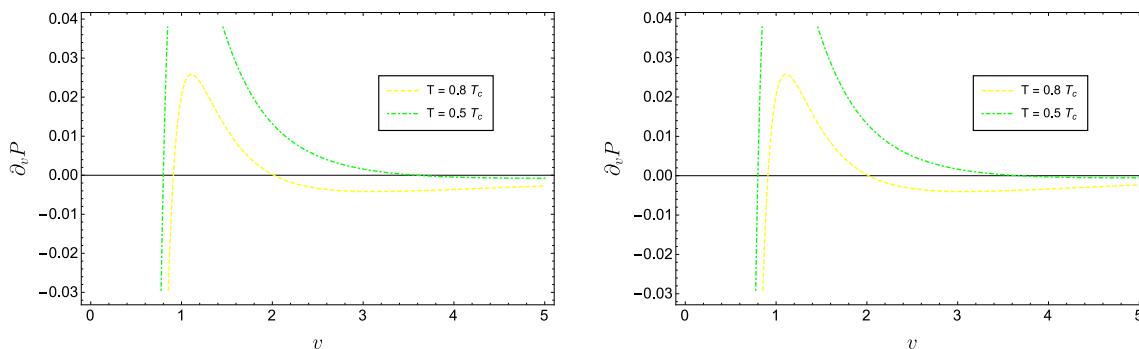


**Figure 7.** Plot of  $\partial_v P$  versus  $v$  for two different values of  $T < T_c$ . We set  $\kappa = 0.01$  (top panel) and  $\kappa = 0.015$  (bottom panel). The two stationary points where  $\partial_v P$  vanishes spot the local minimum and maximum of  $P - v$  curves (online colors).

finally negative again. These ranges are interpreted as the oscillating branch of a van der Waals-like phase transition. The two intermediate points where  $\partial_v P = 0$  represent a local minimum and maximum, respectively (one can further compute the second derivative and check that it is positive in the first point, while negative in the second). Notice also that such stationary points fall within the domain of validity of the expansion (3.8). Indeed, they lie at  $v \lesssim 4 \implies r_+ \lesssim 2$ . This implies that the ratio between the leading order correction and standard term in the expansion (3.8) is of order  $\lesssim \mathcal{O}(10^{-3})$ , thus validating the usage of (3.8).

As  $T$  increases to  $T_c$  (red curve), the oscillating branch squeezes and the two stationary points collapse into the inflection point  $(P_c, v_c, T_c)$  (see eqs. (3.24)–(3.26)). This behaviour is reminiscent of the van der Waals fluid transition. Though not changing the qualitative behavior of the isotherms, Kaniadakis entropy non-trivially affects the critical pressure and temperature at which such transition occurs. For  $T > T_c$  (blue and black curves), there are no more stationary points and  $P$  decreases monotonically along each isotherm as far as  $v$  is small enough to comply with the expansion (3.8). Interestingly enough, from eq. (3.23) one can see that the pressure becomes an increasing function for very large volumes. This behavior appears quite peculiar. On one hand, it may convey the idea that some new physics could emerge in the large-volume limit of Kaniadakis BHs, on the other hand it could simply be the consequence of extrapolating results in a regime where the approximation (3.8) starts becoming less efficient. As pointed out above, understanding the large-volume regime requires much more technical effort and will be postponed to later study.

### 3.3 Gibbs free energy

Let us now explore the global stability of charged AdS BHs in Kaniadakis thermodynamics. For this purpose, we compute the Gibbs free energy as [26, 85]

$$\begin{aligned}
 G(T, P) = M - TS = & \frac{3(Q^2 + r_+^2) + 8\pi P r_+^4}{6r_+} \\
 & + \frac{[Q^2 - r_+^2(1 + 8\pi P r_+^2)]}{4\pi\kappa r_+^3} \tanh(\pi\kappa r_+^2),
 \end{aligned} \tag{3.35}$$

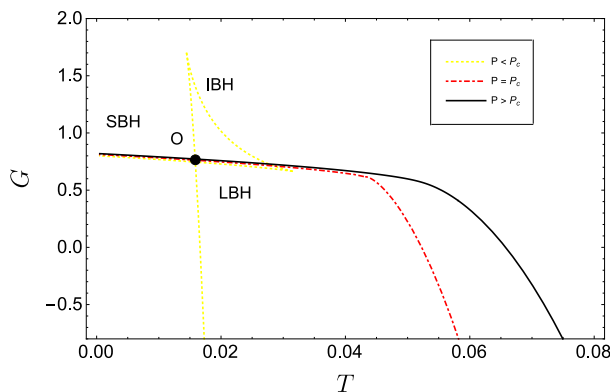


**Figure 8.** The Gibbs free energy  $G$  versus the temperature  $T$ , for  $\kappa = 0.01$ . The red dot-dashed line indicates the critical isobar at  $P = P_c$ . SBH denotes Region I — Small Black Hole, IBH denotes Region II — Intermediate Black Hole and LBH denotes Region III — Large Black Hole, see text (online colors).

where  $r_+$  is to be regarded as a function of  $P$  and  $T$  through the equation of state (3.20). Once more, one can check that the  $\kappa \rightarrow 0$  limit gives back the classical Gibbs free energy for charged AdS BHs

$$G_{\kappa \rightarrow 0}(T, P) = \frac{3Q^2}{4r_+} + \frac{r_+}{4} - \frac{2}{3}\pi P r_+^3. \quad (3.36)$$

The behavior of eq. (3.35) as a function of  $T$  is shown in figure 8, to be compared with figure 2. Consistently with the previous discussion, it is observed that, below the critical pressure (dotted yellow line),  $G$  exhibits has the swallow tail behavior typical of first order phase transitions. Specifically, in the first branch BHs are in the SBH domain. As  $T$  increases to the critical point  $O$ , SBH and LBH phases coexist, since they have the same Gibbs free energy. As noted in [26], the coexistence line in the  $P - T$  plane can be derived by using Maxwell’s equal area law or finding a curve for which  $G$  and  $T$  coincide for SBH and LBH. This line is plainly visible from the 3D plot in figure 9. Above the critical temperature, LBH becomes the preferred thermodynamic state because of its lower Gibbs free energy. Therefore, there is a first-order small-large phase transition at the point  $O$ . Clearly, owing to the definition (1.8) of entropy, different horizon areas for the SBH and LBH during this transition correspond to a discontinuity in the entropy (and also in the thermodynamic volume, see eq. (3.10)) and, thus, to the release of latent heat.

### 3.4 Behavior near the critical point

For quantitative discussion of the behavior of BHs approaching the critical point, we now calculate the critical parameters as defined at the end of section 2. First, we introduce the free energy

$$F(T, V) = G - PV. \quad (3.37)$$

By using eqs. (3.10) and (3.35), we get

$$F = \frac{1}{2} \left[ \frac{Q^2}{r_+} + r_+ - \frac{2T \sinh(\pi\kappa r_+^2)}{\kappa} \right]. \quad (3.38)$$

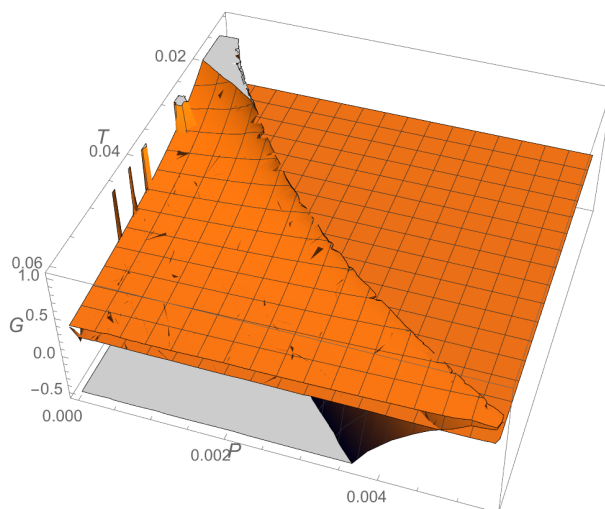


**Figure 9.** 3D plot of the Gibbs free energy  $G$  versus pressure the  $P$  and temperature  $T$ , for  $\kappa = 0.01$ . The coexistence line between the SBH and LBH phases in the  $P - T$  plane is visible.

Accordingly, the entropy is

$$S(T, V) = - \left( \frac{\partial F}{\partial T} \right)_V = \frac{\sinh(\pi\kappa r_+^2)}{\kappa}, \tag{3.39}$$

consistently with eq. (1.8). In turn, from the definition below eq. (2.6), we find that  $C_V = 0$ , which yields  $\alpha = 0$ .

In order to compute  $\beta$ , we approximate eq. (3.30) around a critical point. We use the re-scaled coordinates (2.6), here rewritten for convenience as

$$t = \frac{T}{T_c} - 1, \quad \omega = \frac{V}{V_c} - 1. \tag{3.40}$$

In the approximation of small  $\kappa$ , we obtain

$$p = 1 + \left( \frac{8}{3} - 512\pi^2 Q^4 \kappa^2 \right) t + \left( -\frac{8}{3} + 704\pi^2 Q^4 \kappa^2 \right) t\omega + \left( -\frac{4}{3} + 1120\pi^2 Q^4 \kappa^2 \right) \omega^3 + \mathcal{O}(t\omega^2, \omega^4), \tag{3.41}$$

where the various terms have been grouped together in this specific way for a direct comparison with [26]. It is worth noting that the re-scaled pressure as appears in eq. (3.41) contains terms of order higher than the quadratic in  $\kappa$ , due to the implicit  $\kappa$ -dependence of  $t, \omega$ . However, for our purpose of computing Kaniadakis corrections to critical exponents, it is useful to present eq. (3.41) et seq. in their current form and restore the leading order at the end. For more details on the validity of the series expansion respect to  $t, \omega$ , see [26].

Now, differentiation of eq. (3.41) respect to  $\omega$  at a fixed  $t < 0$  gives

$$dp = \left[ \left( -\frac{8}{3} + 704\pi^2 Q^4 \kappa^2 \right) t + \left( -4 + 3360\pi^2 Q^4 \kappa^2 \right) \omega^2 \right] d\omega. \tag{3.42}$$

By employing Maxwell's equal area law

$$\oint v dP = 0, \quad (3.43)$$

along with the knowledge that there is no pressure variation during the phase transition, we obtain

$$\begin{aligned} & 1 + \left(\frac{8}{3} - 512\pi^2 Q^4 \kappa^2\right) t + \left(-\frac{8}{3} + 704\pi^2 Q^4 \kappa^2\right) t\omega_l + \left(-\frac{4}{3} + 1120\pi^2 Q^4 \kappa^2\right) \omega_l^3 \\ & = 1 + \left(\frac{8}{3} - 512\pi^2 Q^4 \kappa^2\right) t + \left(-\frac{8}{3} + 704\pi^2 Q^4 \kappa^2\right) t\omega_s + \left(-\frac{4}{3} + 1120\pi^2 Q^4 \kappa^2\right) \omega_s^3 \end{aligned} \quad (3.44)$$

and

$$0 = \int_{\omega_l}^{\omega_s} \omega \left[ \left(-\frac{8}{3} + 704\pi^2 Q^4 \kappa^2\right) t + \left(-4 + 3360\pi^2 Q^4 \kappa^2\right) \omega^2 \right] d\omega, \quad (3.45)$$

where  $\omega_{s,l}$  denote the “specific volume” of the small and large phases of BHs, respectively. One can verify that the only non-vanishing solution that reduces to the standard one for  $\kappa \rightarrow 0$  is [26]

$$\omega_s = -\omega_l = \sqrt{-2t} \left(1 + 288\pi^2 Q^4 \kappa^2\right). \quad (3.46)$$

Thus, from the definition of the critical exponent  $\beta$  below eq. (2.6), it follows that

$$\eta = V_c (\omega_l - \omega_s) = 2V_c \omega_l \propto \sqrt{-t} \implies \beta = \frac{1}{2}. \quad (3.47)$$

As concerns the exponent  $\gamma$ , we need to differentiate eq. (3.41) as

$$\left(\frac{dV}{dP}\right)_T = \frac{V_c}{P_c} \left(\frac{d\omega}{dp}\right)_T = -\frac{3}{8} \frac{V_c}{P_c} \frac{1}{t} \left(1 + 264\pi^2 Q^4 \kappa^2\right). \quad (3.48)$$

Hence, the isotherm compressibility  $\kappa_T$  of BHs takes the form

$$\kappa_T = -\frac{1}{V} \left(\frac{\partial V}{\partial P}\right)_T \propto \frac{1}{P_c} \frac{1}{t}, \quad (3.49)$$

which implies  $\gamma = 1$ .

Lastly, the shape of the critical isotherm  $t = 0$  and the related  $\delta$ -exponent are given by

$$p - 1 = \left(-\frac{4}{3} + 1120\pi^2 Q^4 \kappa^2\right) \omega^3 \implies \delta = 3. \quad (3.50)$$

In spite of the non-trivial modifications induced by the  $\kappa$ -deformed entropy to the critical pressure, volume and temperature, the basic critical exponents remain unaffected. This allows to conclude that the qualitative similarity between Kaniadakis BHs and van der Waals fluids near the critical point holds at quantitative level too.

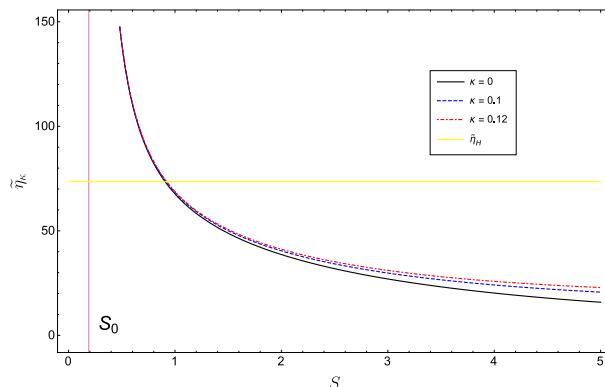


**Figure 10.** The sparsity  $\tilde{\eta}_\kappa$  versus the entropy  $S$ , for various  $\kappa$  and  $l = 2$ . The vertical lines represent the physical limitation entropy  $S_0$  for each curve. For comparison, we have also depicted the sparsity of Schwarzschild BHs with emission of massless bosons (yellow curve) (online colors).

### 3.5 Sparsity of black hole radiation

Although BHs nearly behave like a black body and spontaneously emit particles at a temperature proportional to their surface gravity, the flow of Hawking radiation exhibits some peculiar features. For instance, it is known to be more sparse than black body radiation. Quantitatively speaking, such a difference can be estimated through the computation of the so-called sparsity, which is a measure of the average time-gap between the emission of successive quanta defined by

$$\tilde{\eta} = \frac{C}{g} \left( \frac{\lambda_t^2}{A_{\text{eff}}} \right), \tag{3.51}$$

(we have used the symbol  $\tilde{\eta}$  instead of the traditional  $\eta$  to avoid confusion with the critical exponent (3.47)). Here, the constant  $C$  is dimensionless, while  $g$ ,  $\lambda_t = 2\pi/T$  and  $A_{\text{eff}} = 27\pi r_+^2$  denote the spin degeneracy factor of the emitted quanta, the thermal wavelength and the effective (dimensional) horizon area of the BH, respectively. For Schwarzschild BHs and emission of massless bosons, one has  $\lambda_t = 2\pi/T_H = 8\pi^2 r_+$ , which entails

$$\tilde{\eta}_H = \frac{64\pi^3}{27} \approx 73.49 \gg 1. \tag{3.52}$$

For comparison, we remind that  $\tilde{\eta} \ll 1$  in the case of a black body.

Effects of deformed entropies on sparsity of Schwarzschild BHs have been recently considered in literature (see [64, 86–88] and references therein). For instance, in [64] it has been shown that generalized models of Heisenberg relation combined with non-extensive (Rényi, Tsallis-Cirto, Kaniadakis, Sharma Mittal and Barrow) entropies lead to substantial modifications of the sparsity, which turns out to be mass dependent. A similar statement has been claimed in [88] in rainbow gravity. The question arises as to how such results appear for charged AdS BHs in Kaniadakis framework.

To compute the  $\kappa$ -deformed sparsity, we resort to the definition (3.51) equipped with eq. (3.16). Straightforward calculations yield

$$\tilde{\eta}_\kappa = \tilde{\eta}_H \frac{\pi^2 l^4 \kappa^2 (1 + \kappa^2 S^2) \text{ash}^2(\kappa S)}{\left[ -(\pi l Q \kappa)^2 + \pi l^2 \kappa \text{ash}(\kappa S) + 3 \text{ash}^2(\kappa S) \right]^2}. \tag{3.53}$$

We notice that in the Schwarzschild limit (i.e.  $Q = 0$  and sufficiently large AdS radius  $l$ ), the ensuing expression reduces to the result of [64] for Schwarzschild BHs. By further imposing  $\kappa \rightarrow 0$ , we have  $\tilde{\eta}_\kappa = \tilde{\eta}_H$ , as expected.

The behavior of the  $\kappa$ -modified sparsity (3.53) for various  $\kappa$  and fixed  $l = 2$ ,  $Q = 0.25$  is plotted in figure 10. To better appreciate the difference with respect to the standard case, we have here considered slightly higher values of  $\kappa$  and restricted the range of  $S$  accordingly, so as to keep eq. (3.8) meaningful. We notice that the  $\kappa$ -sparsity shows an apparent divergence for a certain ( $\kappa$ -dependent) value of  $S$ . This singularity, however, lies at the physical limitation point  $S_0$  (see the discussion below eq. (3.16)), as it is easy to understand from the definition (3.51). Thus, it is unphysical and we only have to consider the region  $S > S_0$  delimited by the vertical line. We can see that the  $\kappa$ -deformed sparsity lies always above the  $\kappa = 0$  (black) curve, in such a way that increasing the value of  $\kappa$  directly results in sparser Kaniadakis BH radiation. This is in line with the result of [64]. On the other hand,  $\tilde{\eta}_\kappa$  is greater than the sparsity  $\tilde{\eta}_H$  of Hawking radiation of Schwarzschild BHs (yellow curve) for sufficiently small entropies, where it significantly departs from the black body-like behavior, while it falls below as  $S$  increases.

#### 4 Geometrothermodynamics of charged AdS black holes

Since it is possible to define a temperature for BHs, it is natural to think of an associated substructure. Recently, special care has been devoted to analyze the microscopic constituents and underlying interactions of BHs [10–19], which can be described in the same fashion as the molecules of a non-ideal fluid.

To investigate phenomenologically the nature of interactions among BH microstructures, the common technique consists in studying the thermodynamic geometry of the whole macroscopic system. In this perspective, the analysis of Weinhold [7] and Ruppeiner [8, 9] geometries has proved to give qualitative insights on the internal dynamics of ordinary thermodynamics systems via exploring the sign of the corresponding metric curvature. Specifically, negative (positive) scalar curvatures emerge for prevailing attractive (repulsive) microinteractions, while flatness characterizes non-interacting systems, such as the ideal gas, or systems where interactions are perfectly balanced.

In the effort to probe the character of BH microinteractions, Weinhold and Ruppeiner formalisms have been adapted to BH thermodynamics. This kind of study has been first developed for Banados, Teitelboim and Zanelli (BTZ) BHs [10] and later extended to Reissner-Nordström, Kerr and Reissner-Nordström-AdS BHs [89]. In the plethora of results obtained so far, there is general consensus that the scalar curvature of BH systems with charged molecules should be positive, revealing a repulsive behavior of microinteractions [11–13, 15].

In order to figure out to what extent Kaniadakis' prescription (1.8) affects the above conclusion, let us compute Weinhold and Ruppeiner scalar curvature in Kaniadakis entropy-based thermodynamics. Toward this end, we remind that Weinhold metric is defined as the second derivative of internal energy of the system with respect to given thermodynamic

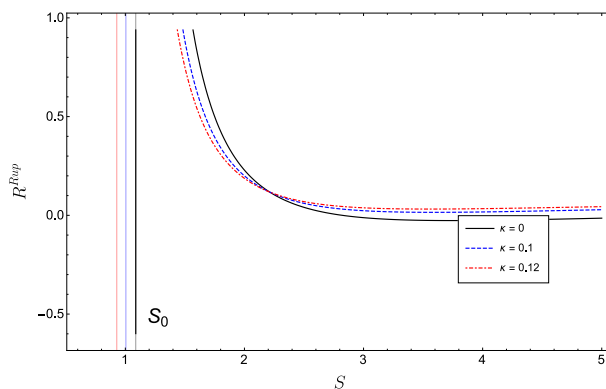


**Figure 11.** The Ruppeiner scalar curvature  $R^{\text{Rup}}$  versus the entropy  $S$ , for various values of  $\kappa$ . The parameter  $l$  is fixed to  $l = \sqrt{2}l_c$  defined through the critical condition (3.26). The vertical lines represent the physical limitation entropy  $S_0$  for each curve (online colors).

variables [7]. For the case of BHs, by identifying the internal energy with the mass, we obtain

$$g_{ij}^w = -\partial_i \partial_j M(S, P, Q) \implies ds_w^2 = g_{ij}^w dx^i dx^j, \quad (4.1)$$

where we have we have generically denoted the independent fluctuation coordinates by  $x^i$ .

Similarly, in Ruppeiner formalism one considers the entropy as basic thermodynamic potential, i.e.

$$g_{ij}^{\text{Rup}} = -\partial_i \partial_j S. \quad (4.2)$$

From eqs. (3.16), (4.1) and (4.2), it follows that the line elements of Weinhold and Ruppeiner are connected each other via the conformal transformation [90]

$$ds_R^2 = \frac{ds_w^2}{T}. \quad (4.3)$$

We focus our next geometrothermodynamic analysis on eq. (4.3). Considering the entropy and pressure as the fluctuation coordinates, while keeping  $Q$  fixed, we obtain the following expression for the Ruppeiner scalar curvature:

$$\begin{aligned} R^{\text{Rup}}(S, P) &= \left(1 + \kappa^2 S^2\right)^{-\frac{1}{2}} [\text{ash}(\kappa S)]^{-1} \\ &\quad \times \kappa^2 \left[-2\pi Q^2 \kappa + \text{ash}(\kappa S)\right] \\ &\quad \times \left\{ \pi (Q\kappa)^2 - \text{ash}(\kappa S) [\kappa + 8P \text{ash}(\kappa S)] \right\}^{-1}, \end{aligned} \quad (4.4)$$

which reduces to the standard curvature for charged AdS BHs in the  $\kappa \rightarrow 0$  limit [13]

$$R_{\kappa \rightarrow 0}^{\text{Rup}}(S, P) = \frac{2\pi Q^2 - S}{S[-\pi Q^2 + S(1 + 8PS)]}. \quad (4.5)$$

The curvature (4.4) versus  $S$  is displayed in figure 11 for various  $\kappa$  and fixed  $Q = 0.6$ ,  $P = 0.5P_c$ . As discussed for the sparsity above, in order to better appreciate the difference

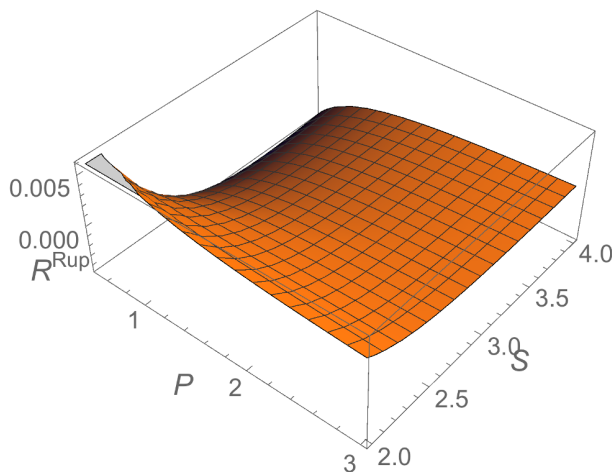


**Figure 12.** 3D plot of the Ruppeiner scalar curvature  $R^{\text{Rup}}$  versus entropy  $S$  and pressure  $P$ , for  $\kappa = 0.1$  and  $Q = 0.6$ .

with respect to the  $\kappa = 0$  case, we have here slightly increased  $\kappa$  and restricted the domain of  $S$  for consistency with the approximation (3.8). Once again, the physical region is delimited by  $S > S_0$  (vertical lines). Although eq. (4.4) is non-trivially modified comparing to the classical curvature, Kaniadakis entropy does not affect the overall sign of  $R^{\text{Rup}}$ , which is still positive and indicates prevailing repulsive interactions among BH microstructures. As  $S$  increases,  $R^{\text{Rup}}$  gradually decreases, which means that the repulsion progressively fades, possibly due to thermal fluctuations and/or molecular collisions. Kaniadakis corrections here manifest through a variation of the rate of decrease, with higher  $\kappa$  corresponding to faster decrease for sufficiently small  $S$ . This tendency is reversed as  $S$  increases. The former behavior resembles the physics of composite systems with non-extensive (and, in particular, superadditive) entropy. Indeed, for such systems the single constituents tend to merge more strongly than the classical extensive case [91], thus balancing swiftly the effects of internal repulsive forces. Asymptotically, the internal microstructures end up being so far apart that  $R^{\text{Rup}} \rightarrow 0$ , which reveals that BHs behave as effectively non-interacting.

Finally, figure 12 shows the 3D plot of  $R^{\text{Rup}}$  versus  $S$  and  $P$  for  $\kappa = 0.1$  and fixed  $Q$  as before. We can see that the scalar curvature remains positive even for varying  $P$ , which supports previous arguments on the repulsive nature of BH micro-interactions.

## 5 Conclusions and discussion

Geometrothermodynamics and phase transitions of charged AdS BHs have been addressed within the framework of Kaniadakis theory, which arises from a self-consistent relativistic generalization of the classical statistical mechanics. The latter is coherently recovered by setting the deformation parameter  $\kappa$  to zero. We would like to stress that the highlight of the present analysis is to deepen our knowledge of BH thermodynamics in a fully relativistic statistical scenario. As far as we know, this is the first work where this scenario is addressed.



Following the standard literature, the study has been conducted by identifying the cosmological constant and its conjugate quantity with the thermodynamic pressure and volume, respectively. In the ensuing extended phase space, we have examined the impact of Kaniadakis entropy on the formal duality black-hole/fluid, showing that Kaniadakis BHs still exhibit a van der Waals-like first order phase transition.

Although Kaniadakis corrections do not affect the qualitative behavior of  $P - v$  diagrams and the basic critical exponents, the critical volume, pressure and temperature are non-trivially modified, even at the leading order in the deformation parameter  $\kappa$  (see eqs. (3.24)–(3.26)). Should we have access to the phenomenology of AdS BHs and measure such quantities, we could elaborate more on the role of Kaniadakis entropy in BH physics and possibly constrain  $\kappa$ -corrections. We have finally probed the nature of interactions among BH micro-structures. Using the picture of fluid-like interacting molecules, we have applied Ruppeiner geometrothermodynamic formalism and computed the scalar curvature of the associated metric. The investigation of the sign of the Ruppeiner scalar curvature  $R^{\text{Rup}}$  reveals that these micro-interactions are prevailing repulsive and tend to vanish for sufficiently large BH horizon radii, with the  $\kappa$ -parameter ruling the rate of decrease. In passing, we mention that a possible explanation for this behavior can be provided based on the physics of the two fluid model, where the dominant character of interactions is determined by the relative number densities of the molecules of the two fluids [13].

As future prospects, we intend to extend the present study beyond the leading order expansion (3.8) of Kaniadakis entropy and possibly develop exact analytic computations of the critical parameters (3.24)–(3.26) and exponents (3.47)–(3.50). Besides technicalities, such an extension could disclose non-trivial features that are peculiar to Kaniadakis AdS BHs and have no correspondence in the standard case. For instance, from the temperature-entropy relation (3.16), we can see that  $T_{\kappa \neq 0}$  becomes a decreasing function for  $S$  large enough and asymptotically vanishes, while the usual expression  $T_{\kappa=0}$  keeps on increasing and finally blows up. In other words, sufficiently large Kaniadakis AdS BHs turn out to be much colder than standard AdS BHs of equal size. Similarly, the equation of state (3.23) shows that the pressure of large AdS BHs is ultimately an increasing function of volume rather than a decreasing one, which could signal interesting new physics in this regime. Unfortunately, a comprehensive examination of these aspects and the related implications on the critical behavior of Kaniadakis AdS BHs lies outside the applicability of the present treatment, since the approximation (3.8) breaks down for entropies large enough. Work is already in progress to settle this issue and will be presented as a future upgrade of this study.

Furthermore, it would be interesting to enrich the above analysis by considering the presence of global monopoles, which are known to have non-trivial effects on BH physics [92–96]. Additionally, one can study Kaniadakis entropy-based thermodynamics of other BHs, such as rotating or exotic BTZ BHs, and additionally examine its effect on the primordial black holes and stochastic gravitational waves [97, 98]. On the other hand, inspired by [64], it is suggestive to understand how BH critical phenomena appear in the context of modified uncertainty principles [99, 100] combined with nonextensive entropies, and possibly connect the two frameworks. The study of these aspects is under active consideration and will be developed elsewhere.

## Acknowledgments

The authors are grateful to the anonymous Reviewer for very helpful suggestions and comments to the original manuscript. GGL would like to thank Jaume Giné, Luca Smaldone and Luca Buoninfante for useful discussions. He is also grateful to the Spanish “Ministerio de Universidades” for the awarded Maria Zambrano fellowship and funding received from the European Union — NextGenerationEU. The authors acknowledge the contribution of the LISA CosWG and of COST Actions CA18108 “Quantum Gravity Phenomenology in the multi-messenger approach” and CA21136 “Addressing observational tensions in cosmology with systematics and fundamental physics (CosmoVerse)”.

**Open Access.** This article is distributed under the terms of the Creative Commons Attribution License ([CC-BY 4.0](https://creativecommons.org/licenses/by/4.0/)), which permits any use, distribution and reproduction in any medium, provided the original author(s) and source are credited.

## References

- [1] S.W. Hawking, *Particle Creation by Black Holes*, *Commun. Math. Phys.* **43** (1975) 199 [*Erratum ibid.* **46** (1976) 206] [[INSPIRE](#)].
- [2] J.D. Bekenstein, *Black holes and entropy*, *Phys. Rev. D* **7** (1973) 2333 [[INSPIRE](#)].
- [3] J.M. Bardeen, B. Carter and S.W. Hawking, *The four laws of black hole mechanics*, *Commun. Math. Phys.* **31** (1973) 161 [[INSPIRE](#)].
- [4] S.W. Hawking and D.N. Page, *Thermodynamics of Black Holes in anti-De Sitter Space*, *Commun. Math. Phys.* **87** (1983) 577 [[INSPIRE](#)].
- [5] S. Capozziello and M. De Laurentis, *Extended Theories of Gravity*, *Phys. Rept.* **509** (2011) 167 [[arXiv:1108.6266](#)] [[INSPIRE](#)].
- [6] R.M. Wald, *The thermodynamics of black holes*, *Living Rev. Rel.* **4** (2001) 6 [[gr-qc/9912119](#)] [[INSPIRE](#)].
- [7] F. Weinhold, *Metric geometry of equilibrium thermodynamics*, *J. Chem. Phys.* **63** (1975) 2479.
- [8] G. Ruppeiner, *Thermodynamics: A Riemannian geometric model*, *Phys. Rev. A* **20** (1979) 1608 [[INSPIRE](#)].
- [9] G. Ruppeiner, *Riemannian geometry in thermodynamic fluctuation theory*, *Rev. Mod. Phys.* **67** (1995) 605.
- [10] R.-G. Cai and J.-H. Cho, *Thermodynamic curvature of the BTZ black hole*, *Phys. Rev. D* **60** (1999) 067502 [[hep-th/9803261](#)] [[INSPIRE](#)].
- [11] S.-W. Wei and Y.-X. Liu, *Insight into the Microscopic Structure of an AdS Black Hole from a Thermodynamical Phase Transition*, *Phys. Rev. Lett.* **115** (2015) 111302 [*Erratum ibid.* **116** (2016) 169903] [[arXiv:1502.00386](#)] [[INSPIRE](#)].
- [12] S.-W. Wei, Y.-X. Liu and R.B. Mann, *Repulsive Interactions and Universal Properties of Charged Anti-de Sitter Black Hole Microstructures*, *Phys. Rev. Lett.* **123** (2019) 071103 [[arXiv:1906.10840](#)] [[INSPIRE](#)].

- [13] X.-Y. Guo, H.-F. Li, L.-C. Zhang and R. Zhao, *Microstructure and continuous phase transition of a Reissner-Nordström-AdS black hole*, *Phys. Rev. D* **100** (2019) 064036 [[arXiv:1901.04703](#)] [[INSPIRE](#)].
- [14] Z.-M. Xu, B. Wu and W.-L. Yang, *Ruppeiner thermodynamic geometry for the Schwarzschild-AdS black hole*, *Phys. Rev. D* **101** (2020) 024018 [[arXiv:1910.12182](#)] [[INSPIRE](#)].
- [15] A. Ghosh and C. Bhamidipati, *Thermodynamic geometry and interacting microstructures of BTZ black holes*, *Phys. Rev. D* **101** (2020) 106007 [[arXiv:2001.10510](#)] [[INSPIRE](#)].
- [16] Z.-M. Xu, B. Wu and W.-L. Yang, *Diagnosis inspired by the thermodynamic geometry for different thermodynamic schemes of the charged BTZ black hole*, *Eur. Phys. J. C* **80** (2020) 997 [[arXiv:2002.00117](#)] [[INSPIRE](#)].
- [17] E. Hirunsirisawat, R. Nakarachinda and C. Promsiri, *Emergent phase, thermodynamic geometry, and criticality of charged black holes from Rényi statistics*, *Phys. Rev. D* **105** (2022) 124049 [[arXiv:2204.13023](#)] [[INSPIRE](#)].
- [18] A. Dehghani, B. Pourhassan, S. Zarepour and E.N. Saridakis, *Thermodynamic schemes of charged BTZ-like black holes in arbitrary dimensions*, *Phys. Dark Univ.* **42** (2023) 101371 [[arXiv:2305.08219](#)] [[INSPIRE](#)].
- [19] F.F. Santos, B. Pourhassan and E. Saridakis, *de Sitter versus anti-de Sitter in Horndeski-like gravity*, [arXiv:2305.05794](#) [[INSPIRE](#)].
- [20] E. Witten, *Anti-de Sitter space and holography*, *Adv. Theor. Math. Phys.* **2** (1998) 253 [[hep-th/9802150](#)] [[INSPIRE](#)].
- [21] A. Chamblin, R. Emparan, C.V. Johnson and R.C. Myers, *Charged AdS black holes and catastrophic holography*, *Phys. Rev. D* **60** (1999) 064018 [[hep-th/9902170](#)] [[INSPIRE](#)].
- [22] A. Chamblin, R. Emparan, C.V. Johnson and R.C. Myers, *Holography, thermodynamics and fluctuations of charged AdS black holes*, *Phys. Rev. D* **60** (1999) 104026 [[hep-th/9904197](#)] [[INSPIRE](#)].
- [23] C. Niu, Y. Tian and X.-N. Wu, *Critical Phenomena and Thermodynamic Geometry of RN-AdS Black Holes*, *Phys. Rev. D* **85** (2012) 024017 [[arXiv:1104.3066](#)] [[INSPIRE](#)].
- [24] A. Sahay, T. Sarkar and G. Sengupta, *Thermodynamic Geometry and Phase Transitions in Kerr-Newman-AdS Black Holes*, *JHEP* **04** (2010) 118 [[arXiv:1002.2538](#)] [[INSPIRE](#)].
- [25] A. Sahay, T. Sarkar and G. Sengupta, *On the Thermodynamic Geometry and Critical Phenomena of AdS Black Holes*, *JHEP* **07** (2010) 082 [[arXiv:1004.1625](#)] [[INSPIRE](#)].
- [26] D. Kubiznak and R.B. Mann, *P-V criticality of charged AdS black holes*, *JHEP* **07** (2012) 033 [[arXiv:1205.0559](#)] [[INSPIRE](#)].
- [27] D. Kastor, S. Ray and J. Traschen, *Enthalpy and the Mechanics of AdS Black Holes*, *Class. Quant. Grav.* **26** (2009) 195011 [[arXiv:0904.2765](#)] [[INSPIRE](#)].
- [28] B.P. Dolan, *The cosmological constant and the black hole equation of state*, *Class. Quant. Grav.* **28** (2011) 125020 [[arXiv:1008.5023](#)] [[INSPIRE](#)].
- [29] B.P. Dolan, *Pressure and volume in the first law of black hole thermodynamics*, *Class. Quant. Grav.* **28** (2011) 235017 [[arXiv:1106.6260](#)] [[INSPIRE](#)].
- [30] T.-F. Gong, J. Jiang and M. Zhang, *Holographic thermodynamics of rotating black holes*, *JHEP* **06** (2023) 105 [[arXiv:2305.00267](#)] [[INSPIRE](#)].

- [31] M.B. Ahmed et al., *Holographic CFT phase transitions and criticality for rotating AdS black holes*, *JHEP* **08** (2023) 142 [[arXiv:2305.03161](#)] [[INSPIRE](#)].
- [32] G. 't Hooft, *Dimensional reduction in quantum gravity*, *Conf. Proc. C* **930308** (1993) 284 [[gr-qc/9310026](#)] [[INSPIRE](#)].
- [33] L. Susskind, *The world as a hologram*, *J. Math. Phys.* **36** (1995) 6377 [[hep-th/9409089](#)] [[INSPIRE](#)].
- [34] C. Tsallis and L.J.L. Cirto, *Black hole thermodynamical entropy*, *Eur. Phys. J. C* **73** (2013) 2487 [[arXiv:1202.2154](#)] [[INSPIRE](#)].
- [35] H. Quevedo, M.N. Quevedo and A. Sanchez, *Quasi-homogeneous black hole thermodynamics*, *Eur. Phys. J. C* **79** (2019) 229 [[arXiv:1812.10599](#)] [[INSPIRE](#)].
- [36] C. Tsallis, *Possible Generalization of Boltzmann-Gibbs Statistics*, *J. Statist. Phys.* **52** (1988) 479 [[INSPIRE](#)].
- [37] J.D. Barrow, *The Area of a Rough Black Hole*, *Phys. Lett. B* **808** (2020) 135643 [[arXiv:2004.09444](#)] [[INSPIRE](#)].
- [38] S. Nojiri, S.D. Odintsov and V. Faraoni, *From nonextensive statistics and black hole entropy to the holographic dark universe*, *Phys. Rev. D* **105** (2022) 044042 [[arXiv:2201.02424](#)] [[INSPIRE](#)].
- [39] A. Rényi, *On the dimension and entropy of probability distributions*, *Acta Math. Acad. Sci. Hung.* **10** (1959) 193.
- [40] B.D. Sharma and D.P. Mittal, *New non-additive measures of relative information*, *J. Comb. Inf. Syst. Sci.* **2** (1977) 122.
- [41] E.N. Saridakis, *Barrow holographic dark energy*, *Phys. Rev. D* **102** (2020) 123525 [[arXiv:2005.04115](#)] [[INSPIRE](#)].
- [42] E.N. Saridakis, K. Bamba, R. Myrzakulov and F.K. Anagnostopoulos, *Holographic dark energy through Tsallis entropy*, *JCAP* **12** (2018) 012 [[arXiv:1806.01301](#)] [[INSPIRE](#)].
- [43] M. Tavayef, A. Sheykhi, K. Bamba and H. Moradpour, *Tsallis Holographic Dark Energy*, *Phys. Lett. B* **781** (2018) 195 [[arXiv:1804.02983](#)] [[INSPIRE](#)].
- [44] G.G. Luciano, *Cosmic evolution and thermal stability of Barrow holographic dark energy in a nonflat Friedmann-Robertson-Walker Universe*, *Phys. Rev. D* **106** (2022) 083530 [[arXiv:2210.06320](#)] [[INSPIRE](#)].
- [45] G.G. Luciano, *From the emergence of cosmic space to horizon thermodynamics in Barrow entropy-based Cosmology*, *Phys. Lett. B* **838** (2023) 137721 [[INSPIRE](#)].
- [46] A. Sheykhi and B. Farsi, *Growth of perturbations in Tsallis and Barrow cosmology*, *Eur. Phys. J. C* **82** (2022) 1111 [[arXiv:2205.04138](#)] [[INSPIRE](#)].
- [47] H. Shababi and K. Ourabah, *Non-Gaussian statistics from the generalized uncertainty principle*, *Eur. Phys. J. Plus* **135** (2020) 697 [[INSPIRE](#)].
- [48] G.G. Luciano, *Tsallis statistics and generalized uncertainty principle*, *Eur. Phys. J. C* **81** (2021) 672 [[INSPIRE](#)].
- [49] G.G. Luciano and M. Blasone, *Nonextensive Tsallis statistics in Unruh effect for Dirac neutrinos*, *Eur. Phys. J. C* **81** (2021) 995 [[arXiv:2107.11402](#)] [[INSPIRE](#)].

- [50] P. Jizba and G. Lambiase, *Tsallis cosmology and its applications in dark matter physics with focus on IceCube high-energy neutrino data*, *Eur. Phys. J. C* **82** (2022) 1123 [[arXiv:2206.12910](#)] [[INSPIRE](#)].
- [51] G. Kaniadakis, *Non-linear kinetics underlying generalized statistics*, *Physica A* **296** (2001) 405.
- [52] G. Kaniadakis, *Statistical mechanics in the context of special relativity*, *Phys. Rev. E* **66** (2002) 056125 [[cond-mat/0210467](#)] [[INSPIRE](#)].
- [53] G. Kaniadakis, *Statistical mechanics in the context of special relativity. II*, *Phys. Rev. E* **72** (2005) 036108 [[cond-mat/0507311](#)] [[INSPIRE](#)].
- [54] G. Kaniadakis, M. Lissia and A.M. Scarfone, *Two-parameter deformations of logarithm, exponential, and entropy: a consistent framework for generalized statistical mechanics*, *Phys. Rev. E* **71** (2005) 046128 [[cond-mat/0409683](#)] [[INSPIRE](#)].
- [55] G. Kaniadakis, P. Quarati and A.M. Scarfone, *Kinetical foundations of non-conventional statistics*, *Physica* **305** (2002) 76 [[cond-mat/0110066](#)] [[INSPIRE](#)].
- [56] G.G. Luciano, *Gravity and Cosmology in Kaniadakis Statistics: Current Status and Future Challenges*, *Entropy* **24** (2022) 1712 [[INSPIRE](#)].
- [57] H. Moradpour, A.H. Ziaie and M. Kord Zangeneh, *Generalized entropies and corresponding holographic dark energy models*, *Eur. Phys. J. C* **80** (2020) 732 [[arXiv:2005.06271](#)] [[INSPIRE](#)].
- [58] A. Lympers, S. Basilakos and E.N. Saridakis, *Modified cosmology through Kaniadakis horizon entropy*, *Eur. Phys. J. C* **81** (2021) 1037 [[arXiv:2108.12366](#)] [[INSPIRE](#)].
- [59] N. Drepanou, A. Lympers, E.N. Saridakis and K. Yesmakhanova, *Kaniadakis holographic dark energy and cosmology*, *Eur. Phys. J. C* **82** (2022) 449 [[arXiv:2109.09181](#)] [[INSPIRE](#)].
- [60] A. Hernández-Almada et al., *Kaniadakis-holographic dark energy: observational constraints and global dynamics*, *Mon. Not. Roy. Astron. Soc.* **511** (2022) 4147 [[arXiv:2111.00558](#)] [[INSPIRE](#)].
- [61] A. Hernández-Almada et al., *Observational constraints and dynamical analysis of Kaniadakis horizon-entropy cosmology*, *Mon. Not. Roy. Astron. Soc.* **512** (2022) 5122 [[arXiv:2112.04615](#)] [[INSPIRE](#)].
- [62] G. Lambiase, G.G. Luciano and A. Sheykhi, *Slow-roll inflation and growth of perturbations in Kaniadakis modification of Friedmann cosmology*, *Eur. Phys. J. C* **83** (2023) 936 [[arXiv:2307.04027](#)] [[INSPIRE](#)].
- [63] E.M.C. Abreu, J. Ananias Neto, E.M. Barboza and R.C. Nunes, *Jeans instability criterion from the viewpoint of Kaniadakis' statistics*, *EPL* **114** (2016) 55001 [[arXiv:1603.00296](#)] [[INSPIRE](#)].
- [64] I. Cimidiker, M.P. Dabrowski and H. Gohar, *Generalized uncertainty principle impact on nonextensive black hole thermodynamics*, *Class. Quant. Grav.* **40** (2023) 145001 [[arXiv:2301.00609](#)] [[INSPIRE](#)].
- [65] A. Kempf, G. Mangano and R.B. Mann, *Hilbert space representation of the minimal length uncertainty relation*, *Phys. Rev. D* **52** (1995) 1108 [[hep-th/9412167](#)] [[INSPIRE](#)].
- [66] G.G. Luciano and L. Petruzzello, *Generalized uncertainty principle and its implications on geometric phases in quantum mechanics*, *Eur. Phys. J. Plus* **136** (2021) 179 [[INSPIRE](#)].

- [67] T.S. Biró and V.G. Czinner, *A  $q$ -parameter bound for particle spectra based on black hole thermodynamics with Rényi entropy*, *Phys. Lett. B* **726** (2013) 861 [[arXiv:1309.4261](#)] [[INSPIRE](#)].
- [68] V.G. Czinner and H. Iguchi, *Thermodynamics, stability and Hawking-Page transition of Kerr black holes from Rényi statistics*, *Eur. Phys. J. C* **77** (2017) 892 [[arXiv:1702.05341](#)] [[INSPIRE](#)].
- [69] S. Ghaffari et al., *Black hole thermodynamics in Sharma-Mittal generalized entropy formalism*, *Gen. Rel. Grav.* **51** (2019) 93 [[arXiv:1901.01506](#)] [[INSPIRE](#)].
- [70] H. Moradpour, A.H. Ziaie and C. Corda, *Tsallis uncertainty*, *Europhys. Lett.* **134** (2021) 20003.
- [71] H. Moradpour et al., *The third law of thermodynamics, non-extensivity and energy definition in black hole physics*, *Mod. Phys. Lett. A* **37** (2022) 2250076 [[arXiv:2106.00378](#)] [[INSPIRE](#)].
- [72] S. Nojiri, S.D. Odintsov and V. Faraoni, *Area-law versus Rényi and Tsallis black hole entropies*, *Phys. Rev. D* **104** (2021) 084030 [[arXiv:2109.05315](#)] [[INSPIRE](#)].
- [73] S. Nojiri, S.D. Odintsov and V. Faraoni, *Alternative entropies and consistent black hole thermodynamics*, *Int. J. Geom. Meth. Mod. Phys.* **19** (2022) 2250210 [[arXiv:2207.07905](#)] [[INSPIRE](#)].
- [74] N. Goldenfeld, *Lectures on phase transitions and the renormalization group*, CRC Press (1992) [[DOI:10.1201/9780429493492](#)] [[INSPIRE](#)].
- [75] H. Reissner, *Über die eigengravitation des elektrischen felde nach der einsteinschen theorie*, *Annalen Phys.* **355** (1916) 106.
- [76] E.N. Saridakis, *Modified cosmology through spacetime thermodynamics and Barrow horizon entropy*, *JCAP* **07** (2020) 031 [[arXiv:2006.01105](#)] [[INSPIRE](#)].
- [77] S. Rani, A. Jawad, H. Moradpour and A. Tanveer, *Tsallis entropy inspires geometric thermodynamics of specific black hole*, *Eur. Phys. J. C* **82** (2022) 713 [[INSPIRE](#)].
- [78] A. Jawad and S.R. Fatima, *Thermodynamic geometries analysis of charged black holes with barrow entropy*, *Nucl. Phys. B* **976** (2022) 115697 [[INSPIRE](#)].
- [79] G.G. Luciano and A. Sheykhi, *Black hole geometrothermodynamics and critical phenomena: A look from Tsallis entropy-based perspective*, *Phys. Dark Univ.* **42** (2023) 101319 [[arXiv:2304.11006](#)] [[INSPIRE](#)].
- [80] S. Basilakos, A. Lymperis, M. Petronikolou and E.N. Saridakis, *Alleviating both  $H_0$  and  $\sigma_8$  tensions in Tsallis cosmology*, [arXiv:2308.01200](#) [[INSPIRE](#)].
- [81] F. Jüttner, *Das maxwellsche gesetz der geschwindigkeitsverteilung in der relativtheorie*, *Annalen Phys.* **339** (1911) 856.
- [82] G.G. Luciano, *Modified Friedmann equations from Kaniadakis entropy and cosmological implications on baryogenesis and  ${}^7\text{Li}$ -abundance*, *Eur. Phys. J. C* **82** (2022) 314 [[INSPIRE](#)].
- [83] C.H. Nam, *Non-linear charged AdS black hole in massive gravity*, *Eur. Phys. J. C* **78** (2018) 1016 [[INSPIRE](#)].
- [84] G.A. Marks, F. Simovic and R.B. Mann, *Phase transitions in 4D Gauss-Bonnet-de Sitter black holes*, *Phys. Rev. D* **104** (2021) 104056 [[arXiv:2107.11352](#)] [[INSPIRE](#)].



- [85] G.-M. Deng, J. Fan, X. Li and Y.-C. Huang, *Thermodynamics and phase transition of charged AdS black holes with a global monopole*, *Int. J. Mod. Phys. A* **33** (2018) 1850022 [[arXiv:1801.08028](#)] [[INSPIRE](#)].
- [86] A. Alonso-Serrano, M.P. Dabrowski and H. Gohar, *Nonextensive Black Hole Entropy and Quantum Gravity Effects at the Last Stages of Evaporation*, *Phys. Rev. D* **103** (2021) 026021 [[arXiv:2009.02129](#)] [[INSPIRE](#)].
- [87] A. Alonso-Serrano, M.P. Dabrowski and H. Gohar, *Minimal length and the flow of entropy from black holes*, *Int. J. Mod. Phys. D* **27** (2018) 1847028 [[arXiv:1805.07690](#)] [[INSPIRE](#)].
- [88] Z.-W. Feng, X. Zhou, S.-Q. Zhou and D.-D. Feng, *Rainbow gravity corrections to the information flux of a black hole and the sparsity of Hawking radiation*, *Annals Phys.* **416** (2020) 168144 [[arXiv:1808.09958](#)] [[INSPIRE](#)].
- [89] J.-Y. Shen, R.-G. Cai, B. Wang and R.-K. Su, *Thermodynamic geometry and critical behavior of black holes*, *Int. J. Mod. Phys. A* **22** (2007) 11 [[gr-qc/0512035](#)] [[INSPIRE](#)].
- [90] R. Mrugała, *On equivalence of two metrics in classical thermodynamics*, *Physica A* **125** (1984) 631.
- [91] P.T. Landsberg and V. Vedral, *Distributions and channel capacities in generalized statistical mechanics*, *Phys. Lett. A* **247** (1998) 211.
- [92] J.-L. Jing, H.-W. Yu and Y.-J. Wang, *Thermodynamics of a black hole with a global monopole*, *Phys. Lett. A* **178** (1993) 59 [[INSPIRE](#)].
- [93] H.-W. Yu, *Black hole thermodynamics and global monopoles*, *Nucl. Phys. B* **430** (1994) 427 [[INSPIRE](#)].
- [94] X.-Z. Li and J.-G. Hao, *Global monopole in asymptotically dS / AdS space-time*, *Phys. Rev. D* **66** (2002) 107701 [[hep-th/0210050](#)] [[INSPIRE](#)].
- [95] Q.-Q. Jiang and S.-Q. Wu, *Hawking radiation of charged particles as tunneling from Reissner-Nordström-de Sitter black holes with a global monopole*, *Phys. Lett. B* **635** (2006) 151 [[hep-th/0511123](#)] [[INSPIRE](#)].
- [96] T.R.P. Caramês, J.C. Fabris, E.R. Bezerra de Mello and H. Belich,  *$f(R)$  global monopole revisited*, *Eur. Phys. J. C* **77** (2017) 496 [[arXiv:1706.02782](#)] [[INSPIRE](#)].
- [97] T. Papanikolaou, A. Lymperis, S. Lola and E.N. Saridakis, *Primordial black holes and gravitational waves from non-canonical inflation*, *JCAP* **03** (2023) 003 [[arXiv:2211.14900](#)] [[INSPIRE](#)].
- [98] S. Basilakos et al., *Gravitational wave signatures of no-scale Supergravity in NANOGrav and beyond*, [arXiv:2307.08601](#) [[INSPIRE](#)].
- [99] S. Mignemi, *Extended uncertainty principle and the geometry of (anti)-de Sitter space*, *Mod. Phys. Lett. A* **25** (2010) 1697 [[arXiv:0909.1202](#)] [[INSPIRE](#)].
- [100] J. Giné and G.G. Luciano, *Modified inertia from extended uncertainty principle(s) and its relation to MoND*, *Eur. Phys. J. C* **80** (2020) 1039 [[INSPIRE](#)].